Holocene Cyclic Records of Ice-Rafted Debris and Sea Ice Variations on the East Greenland and Northwest Iceland Margins

Authors: Darby, D. A., Andrews, J. T., Belt, S. T., Jennings, A. E., and Cabedo-Sanz, P.

Source: Arctic, Antarctic, and Alpine Research, 49(4) : 649-672

Published By: Institute of Arctic and Alpine Research (INSTAAR), University of Colorado

URL: https://doi.org/10.1657/AAAR0017-008

Arctic, Antarctic, and Alpine Research, Vol. 49, No. 4, 2017, pp. 649–672
DOI: http://dx.doi.org/10.1657/AAAR0017-008

Holocene cyclic records of ice-rafted debris and sea ice variations on the East Greenland and Northwest Iceland margins

D. A. Darby[1,*], J. T. Andrews[2], S. T. Belt[3], A. E. Jennings[2], and P. Cabedo-Sanz[3]

[1]Department of Ocean, Earth, and Atmospheric Sciences, Old Dominion University, Norfolk, Virginia 32529, U.S.A.
[2]INSTAAR *and* Department of Geological Sciences, University of Colorado, UCB 450, Boulder, Colorado 80309-0450, U.S.A.
[3]Biogeochemistry Research Centre, School of Geography, Earth and Environmental Sciences, University of Plymouth, Drake Circus, Plymouth, PL4 8AA, U.K.
[*]Corresponding author's email: ddarby@odu.edu

A B S T R A C T

The dynamics of the Greenland Ice Sheet and drift of sea ice from the Arctic Ocean reaching Denmark Strait are poorly constrained. We present data on the provenance of Fe oxide detrital grains from two cores in the Denmark Strait area and compare the Fe grain source data with other environmental proxies in order to document the variations and potential periodicities in ice-rafted debris delivery during the Holocene. Based on their Fe grain geochemistry, the sediments can be traced to East Greenland sources and to more distal sites around the Arctic Basin. On the Holocene time scales of the two cores, sea ice biomarker (IP_{25}) data, and quartz weight percent reveal positive associations with T°C and inverse associations with biogenic carbonate wt%. Trends in the data were obtained from Singular Spectrum Analysis (SSA), and residuals were tested for cyclicity. Trends on the environmental proxies explained between 15 and 90% of the variance. At both sites the primary Fe grain sources were from Greenland, but significant contributions were also noted from Banks Island and Svalbard. There is a prominent cyclicity of 800 yrs as well as other less prominent cycles for both Greenland and arctic sources. The Fe grain sources from Greenland and the circum–Arctic Ocean are in synchronization, suggesting that the forcings for these cycles are regional and not local ice sheet instabilities.

Introduction

Marine sediment cores from the continental margin of East Greenland and NW Iceland have the potential to document changes in sediment transport and provenance from both Greenland-derived icebergs and sediments entrained in sea ice (ice-rafted debris; IRD) originating on the shallow shelves around the Arctic Basin (Nam et al., 1995; Stein et al., 1993). Recently documented mass losses in the Greenland Ice Sheet (GIS), local Greenland glaciers, and ice caps (Shepherd and Wingham, 2007; Seale et al., 2011; Khan et al., 2015), and reductions in the volume and area of arctic sea ice (Meier et al., 2005; Stroeve et al., 2012) suggest that it is critical to evaluate these recent changes (of the past 1–2 decades) against longer paleoclimate time series. In this paper we present new data on the variations in Fe oxide grains (250 μm to 45 μm) (Darby et al., 2015) and compare those data with sea ice biomarker (IP_{25}) data (Belt et al., 2007; Belt and Müller, 2013) and other paleoclimate proxies from cores MD99-2322 (henceforth 2322) and MD99-2263 (henceforth 2263) (Fig. 1) from either side of Denmark Strait. Both cores have a rich variety of other previously published climate and sediment proxies that are used to compare with the Fe grain source data and IP_{25} data to provide a robust paleoceanographic context. Core 2322

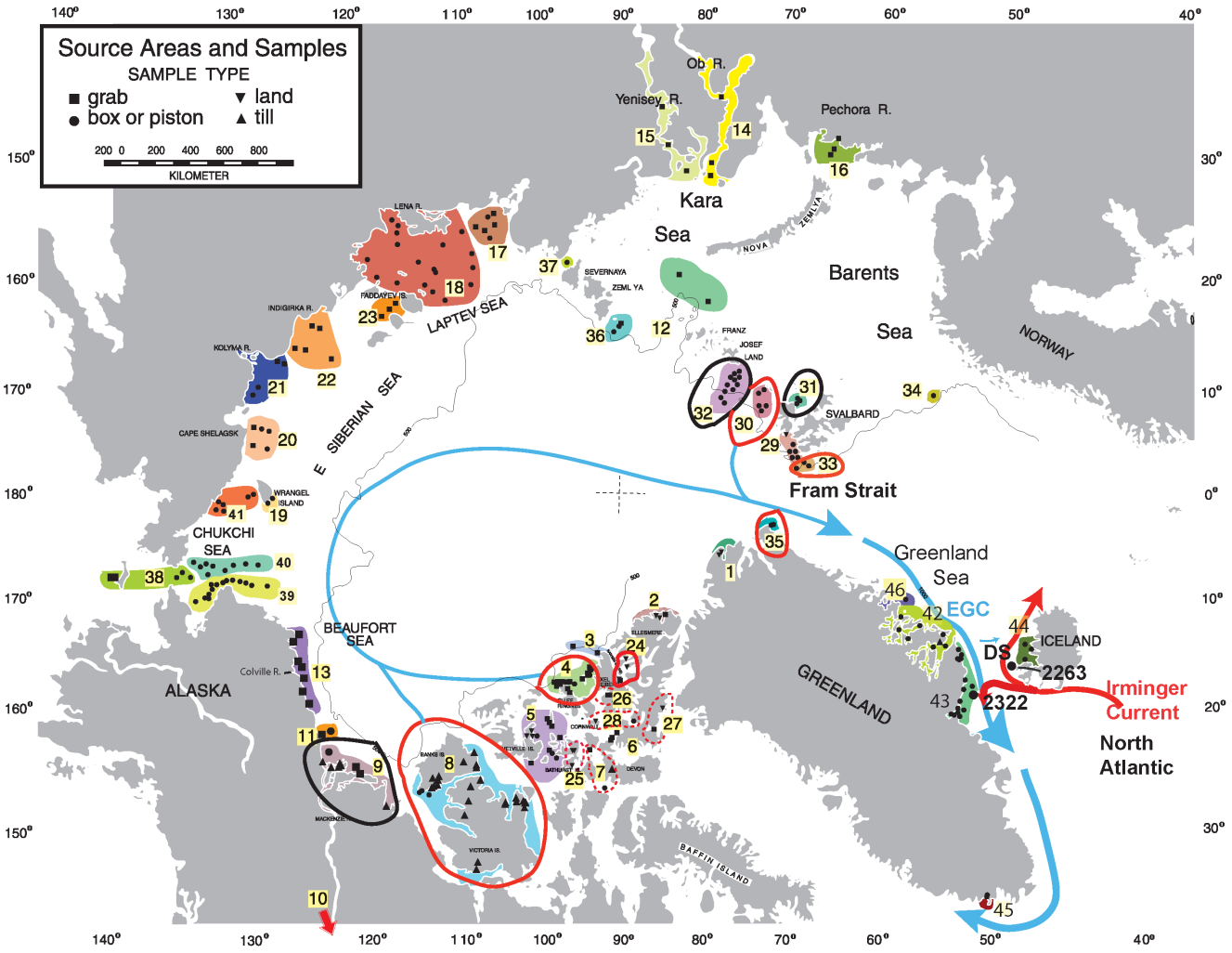

FIGURE 1. Circum-Arctic and Greenland source areas (1–46) and location of cores 2322 and 2263 at Denmark Strait (DS). The circum-Arctic sources for core 2322 that supplied more than 1.5 Fe grains in any sample are circled in black, whereas those that delivered more than 3 Fe grains are circled in red. Cold Arctic and East Greenland Currents (EGC) are in blue, whereas the warm Irminger Current (IC) is in red.

is a very well-dated Holocene core that we analyzed to 11 cal ka B.P. (Stoner et al., 2007; Jennings et al., 2011), whereas 2263 is a box core that extends back to ca. 2 cal ka B.P., also with excellent age control (Andrews et al., 2009a).

The interpretation of sediment records associated with sea ice and iceberg rafting is that changes usually are caused by variations in the quantity of drift ice, including increased iceberg calving (Ruddiman, 1977b). However, several studies (Warren, 1992; Andrews, 2000; Clark and Pisias, 2000) have pointed out that changes in IRD also may be caused by changes in: (1) sediment entrainment at the source (glacier or sea ice), (2) the direction of transport (i.e. drift), (3) the rate of melting of the drift ice, and (4) the mass transport of drift ice (sea ice and icebergs), as well as a combination of any of these. Using the climate proxies that exist for the studied cores, including summer surface sea-temperature estimates based on planktic foraminiferal assemblages in core 2322 (Jennings et al., 2011) and bottom water temperature estimates based on benthic foraminiferal assemblages (**Ólafsdóttir** et al., 2010) (both referred to as T°C) and sea ice estimates (Andrews et al., 2009a; Jennings et al., 2011), we evaluate how the Fe grain source variations are related to estimates of changes in sea ice and ocean temperature, and present information on the trends and cycles evident in these new data. On Late Quaternary time scales, Ruddiman (1977a) linked increases in IRD deposition with ocean temperatures and iceberg melting, whereas others (Bugelmayer-Blaschek et al., 2016) concluded that "internal ice sheet variability seems to be the source of the multi-century and millennial-scale iceberg events during the Holocene."

Oceanographic Circulation and Environment

The modern surface circulation regime along East Greenland and in the Denmark Strait influences where we expect icebergs and sea ice to drift, melt, and release their sediment load. The East Greenland Current (EGC) is a continuation of the Trans Polar Drift, which flows out of the Arctic Ocean, through the Fram Strait, and along the full length of eastern Greenland. It transports ice from the Arctic Ocean and is augmented along its path by icebergs and freshwater released from local glaciers and GIS outlets (Hastings, 1960; Rudels et al., 2002; Sutherland and Pickart, 2008) (Fig. 1). The EGC bifurcates into two branches north of Denmark Strait. The main current travels along the Greenland margin, and a second separates from it at the northern end of the Blosseville Basin just south of Scoresby Sund, and joins the North Iceland Jet on the Icelandic slope before passing over the Denmark Strait (Våge et al., 2013). The relatively warm and saline Irminger Current (IC), a branch of the North Atlantic Current, flows northward along the western Iceland shelf toward the Djúpáll Trough and then bends around N Iceland as the North Iceland Irminger Current (Malmberg, 1985). Where the EGC and IC meet in the Denmark Strait is a local expression of the marine Polar Front where there is enhanced melting of drift ice, resulting in release of their entrained sediment (Jennings et al., 2014). The IC bifurcates south of the Denmark Strait, and eddies shed from this warm current (Kraus, 1958) penetrate into the fjords to impact the grounding lines of the GIS outlet glaciers here (Fig. 1) (Straneo and Heimbach, 2013).

Fast ice forms in the fjords and along the coast of Greenland and in severe years forms a sea ice/iceberg mélange (siqussaq) that effectively locks icebergs in the fjords and may act to stabilize the outlet glaciers (Reeh et al., 2001; Amundson et al., 2010). Strong katabatic winds off the ice sheet may break up the siqussaq and release the icebergs from the fjords into the EGC (Straneo and Heimbach, 2013; Moore and Renfrew, 2014). The offshore sea ice covers the site of 2322 for 6.5 to 8.5 months per yr (Jennings et al., 2011). Core 2263 is located several kilometers seaward of the average position of the ice edge between A.D. 1870 and 1920 (Divine and Dick, 2006). In January 2007, sea ice extended across Djúpáll and reached the Westfirdir coast (Jónsdóttir and Sveinbjornsson, 2007). Historical data (Ogilvie, 1996; Ogilvie and Jónsdóttir, 2000) indicate the presence of sea ice during severe climatic intervals (Wallevik and Sigurjónsson, 1998), and the historic flux of storis (arctic sea ice that is transported to Southwest and West Greenland) through the Fram Strait (Schmith and Hanssen, 2003) closely match the drift ice records on the Iceland shelf (Alonso-Garcia et al., 2013).

There are no official counts of icebergs through time along the E Greenland shelf, although icebergs present a danger to shipping and as such are presently reported in the Icelandic Meteorological Office web site (http://www.hafro.is). An unusual concentration of icebergs occurred in Icelandic waters during August 2004 and September 2011 (Appendix Figs. A1 and A2). Bigg (1999) estimated a flux of 25 km^3/yr from the tidewater glaciers north of Scoresby Sund (Area 2 in Fig. 2, part A), whereas fluxes of 2 and 18 km^3/yr were estimated for the tidewater glaciers in Nansen and Kangerlussuaq fjords (Andrews et al., 1994), near core 2322 (Area 3 in Fig. 2, part A). In the past decade or so, the iceberg flux has probably increased (van den Broeke et al., 2009; Kjeldsen et al., 2015).

Sediment Cores

Core 2322 (67.136°N, 30.827°W, 714 m water depth [wd]) (Labeyrie et al., 2003) was selected because of its location on the southeastern shelf of Greenland in the path of the EGC. It has a relatively high average sedimentation rate of 1 m/kyr for the upper 7 kyr to more than 5 m/kyr below this, and an excellent age model based on 20 calibrated radiocarbon dates and paleomagnetic data (Stoner et al., 2007; Jennings et al., 2011). Shipboard observations in 1991 and 1993 along the Geikie Plateau and in Kangerlussuaq Fjord indicated individual icebergs with supraglacial, englacial, or basal debris, which was especially evident for icebergs calved within the area of basalt outcrop, and aerial photographs showed that many of the glaciers on the Geikie Plateau had supraglacial sediment loads. Core 2322 was sampled for Fe grain analyses at 10.5 cm intervals in the upper 7 kyr (820 cm), compared to an average 30 cm interval below this in order to achieve a median age interval between samples of 70–80 yrs. Near surface, summer sea surface temperatures were estimated from planktic foraminiferal assemblages at about 100-yr intervals, and grain size data pertinent to IRD deposition (>1 mm, 1 mm–106 μm, and 106–63 μm wt% data) were measured on average every 20 yrs throughout the core (Jennings et al., 2011). Mineralogy (X-Ray Diffraction, qXRD) was previously analyzed at about 100-yr intervals (Andrews et al., 2014) and at 30-yr resolution for the last 2 cal ka B.P. (Andrews and Jennings, 2014). IP_{25} data were obtained with a mean 100-yr resolution for the past 8 cal ka B.P.

Box core 2263 (66.679°N, 24.196°W, 235 m wd) (Fig. 2, part A) was collected from the center of a large sediment drift in Djúpáll Trough (Geirsd**ó**ttir et al., 2002;

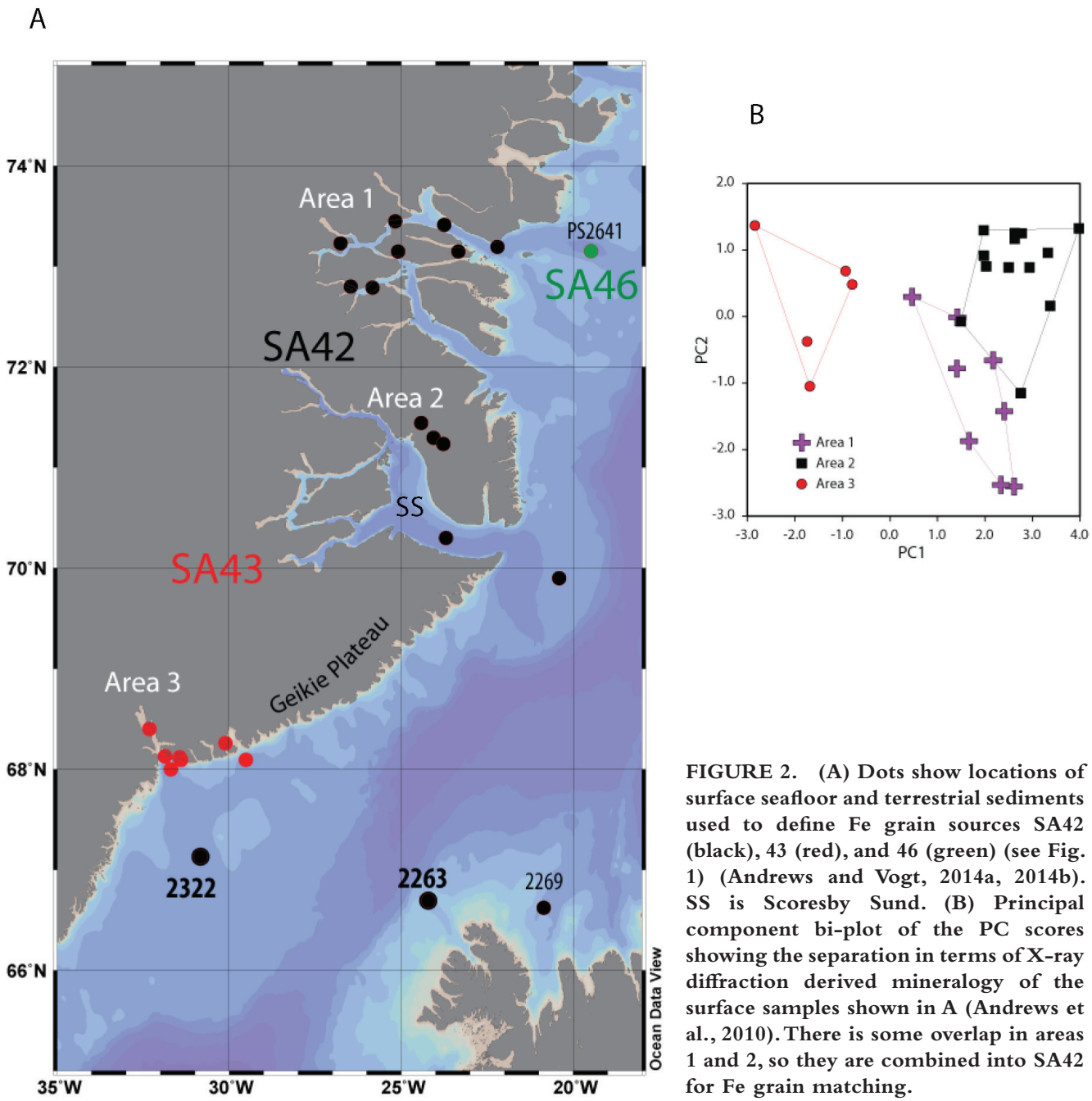

FIGURE 2. (A) Dots show locations of surface seafloor and terrestrial sediments used to define Fe grain sources SA42 (black), 43 (red), and 46 (green) (see Fig. 1) (Andrews and Vogt, 2014a, 2014b). SS is Scoresby Sund. (B) Principal component bi-plot of the PC scores showing the separation in terms of X-ray diffraction derived mineralogy of the surface samples shown in A (Andrews et al., 2010). There is some overlap in areas 1 and 2, so they are combined into SA42 for Fe grain matching.

Ólafsdóttir, 2004) that extends from Ísafjardardjúp to the shelf break adjacent to Denmark Strait (Labeyrie et al., 2003; Andrews et al., 2009a; **Ólafsdóttir** et al., 2010). The site of core 2263 lies beneath the axis of the warm IC. Late Holocene foraminiferal faunas are dominated by boreal species at this site (Jennings et al., 2004; **Ólafsdóttir** et al., 2010). In the past decade, the February 50 m temperatures over the site are in the range of 3–6 °C, indicating a dominance of IC water at the site (http://www.hafro.is). Today, Djúpáll is close to but beyond the southern limit of drift ice as shown by the absence of quartz and IP_{25} from surface samples on the West Iceland shelf (Axford et al., 2011; Cabedo-Sanz et al., 2016). However, historically, polar surface water and drift ice have moved onto the Northwest Iceland shelf (Koch, 1945; Ogilvie, 1997; Divine and Dick, 2006), and mineralogical evidence of this advection has been documented in Holocene sediment cores (Andrews et al., 2009b). Core 2263 has seven radiocarbon dates plus ^{210}Pb and ^{137}Cs data that make a reasonable age model for the past two millennia (Andrews et al., 2009a). It was sampled every centimeter to the bottom of the box core at 46 cm (age interval of 12–50 yrs per sample). A variety of published paleoclimate proxies have been

documented for this site, including T°C, IP_{25}, carbonate content, grain size, and quartz wt% (NOAA Paleoclimate Database, https://www.ncdc.noaa.gov/paleo/study/16398).

Methods Background: Geology, Fe Grain Sourcing, IP_{25}, and Data Analysis

There are several distinct proximal Fe grain source areas (SA) for Denmark Strait IRD that include East and Southeast Greenland and Northwest Iceland (SA42, 43, 44, and 46; Figs. 1 and 2, part A). SA46 comprises several samples in the same sediment core from the Kejser Franz Joseph Trough (PS2641; Fig. 2, part A). As this source might include IRD from farther north transported by the EGC, Fe grains matched to arctic sources were removed from the data set for this source so that the remaining Fe grains represent local sources. All of the source areas shown in Figure 1 were constructed based primarily on geographic grounds but also with differences in rock types and mineralogy of the samples in each source area (Darby and Bischof, 1996). Most source areas contain a natural cluster of samples within a geographic area and have common source rock lithologies, even though similar lithologies also occur in other source areas. As shown earlier (Darby et al., 2015), in all cases the Fe grain geochemical compositions of each source area are unique regardless of the source rock lithologies.

SA42 comprises a series of samples from the fjords that extend into the Caledonian outcrop (Hubberten, 1995; Higgins et al., 2008), and the region of SA43 consists of till samples from the northern flank of Scoresby Sund derived from the erosion of Precambrian granite gneiss (Lysa and Landvik, 1994) and samples further south that are derived from erosion of the early Tertiary East Greenland flood basalts of the Geikie Plateau (Brooks, 1990; Stein, 1996; Larsen et al., 1999; Brooks, 2008), including the Skaergaard Intrusion (McBirney and Noyes, 1979). The SA43 sites in Kangerlussuaq Fjord also have sediments derived from erosion of Archean granite gneisses, whereas sites around Nansen Fjord would also record similar mineralogy because they were eroded from Cretaceous sandstones and siltstones derived from the Archean gneisses with little alteration (Larsen et al., 1999; Andrews, unpublished data). Finally, we include samples from the northwest Iceland shelf as SA44 (Fig. 1). These represent mostly sea ice IRD deposits from Iceland and foreign IRD from sources farther north that might be ice rafted into these waters. This source area is down-drift from core 2263, and Fe grains matched to this source are not seen in this core. As such SA44 is not considered further here.

The designation of Fe grain sources was, as noted above, largely based on geographic area. To test whether the Fe grain samples from SA42, 43, and 46 are indeed mineralogically distinct we calculated Principal Component (PC) scores on the log-ratio-transformed wt% qXRD data (Aitchison, 1986) from many of the same samples used for Fe grain analysis (Andrews and Vogt, 2014a, 2014b). The resulting PC scores defined three areas of Greenland with distinct mineral compositions (Fig. 2, part B). SA43 is distinct mineralogically (Area 3), but SA42 consists of both areas 1 and 2 as defined by the qXRD (Fig. 2, parts A and B); SA46 is a mixture of sediments derived from west of PS2641 (Fig. 2, part A) (Andrews et al., 2016).

The Fe grains from both core samples and source area samples were separated from sieved samples using a hand magnet and the Frantz magnetic separator (Darby et al., 2015). The magnetic fraction in the range 250 to 45 μm (250 to 63 μm in the case of core 2322) was mounted in one-inch epoxy molds, polished, labeled, and photographed for easy location of grains during micro-probe analyses. Each Fe grain was identified under 1000× reflected-light microscopy, and this mineralogy, after it was corrected using the elemental composition from the micro-probe analyses, was used to help match grains to source Fe grains of the same mineralogy. Anhydrous Fe oxide mineral grains (Fe grains) were used for source determination because these minerals incorporate large amounts of foreign elements into their crystal lattice during formation in metamorphic or igneous processes (Haggerty, 1976). We used 14 elements to precisely match each Fe grain to a near exact composition in analyzed source areas (Darby et al., 2015). Besides Fe, O, and Ti, we analyzed for Mn, Mg, Si, Al, Ca, Zn, V, Ni, Cr, Nb, and Ta using a Cameca SX100 electron probe microanalyzer. Each element was matched in turn to the same element analyzed from source area sample Fe grains of the same mineralogy using two standard deviations on replicate analyses of grains of the same mineralogy. Each Fe grain can match to more than one source if the chemical criteria for matching are met. Where this occurs, the Fe grain was matched to each source area by pro-rationing by closeness of composition. So if the sum of element differences between one source Fe grain is 0.5% and the second is 1%, the first source area would get a match of 0.67 and the second a match of 0.33. Thus a core sample Fe grain might match into more than one source area, but the sum of all its matches is one. This further decreases errors of mismatch by including all source areas that meet the match criteria for all 14 elements. All matches for all mineral types to a

source area were summed, and this number, divided by the dried sediment weight of the sample (average = 15.5 ± 6.4 g) from the core is reported here as Fe grains/g for 2322 (Fig. 3). This number was corrected for the number of Fe grains not analyzed in each sample so, for example, where only 100 Fe grains were analyzed and there were 150 Fe grains, all sources were multiplied by 1.5. Because dry sample weights were not available in 2263, only the number of Fe grains matched to each source is reported. This matching protocol has been extensively tested where all 37,000 Fe grain analyses from the source data set were matched to all grains of the same data set except the same grain and the error in matching was 1.5%. This data set is published in Darby et al. (2015) and is archived in the Snow and Ice Data Center, Boulder, Colorado, as indicated in Darby et al. (2015).

The sea ice biomarker IP_{25} has been shown to be present in surface sediments from regions of northern Iceland experiencing drift ice in recent decades (Cabedo-Sanz et al., 2016), and IP_{25} abundances in the past millennial down-core records align well with observational sea ice records (Massé et al., 2008, Andrews et al., 2009a). Such ground-truthing of this drift ice proxy has recently enabled a Holocene sea ice reconstruction for sites from the north Icelandic Shelf (Cabedo-Sanz et al., 2016). Further, Alonso-Garcia et al. (2013) demonstrated that IP_{25} abundances in short cores from the East Greenland Shelf (and close to core 2322) likely reflected changes in drift ice delivery within Denmark Strait.

Key interests of our study were to see if (1) there are significant trends in both the source area data from cores 2322 and 2263 and in ocean climate proxies that we might expect to co-vary with those data (such as IP_{25} or T°C estimates); and (2) there is evidence for multi-century cycles in the Fe grain sources. Such cycles have been predicted on the basis of models of internal ice sheet variability (Bugelmayer-Blaschek et al., 2016), but also could be associated with periods of enhanced melting of drift ice in Denmark Strait at the marine polar front (Jennings et al., 2014) or surges in icebergs released to Denmark Strait from siqussaq break-up in the fjords (Straneo and Heimbach, 2013; Moore and Renfrew, 2014).

To undertake these studies, we first derived equi-spaced samples using the AnalySeries integration option (Paillard et al., 1996), making sure to oversample so as to reduce interpolation. Given the varied sampling intervals of our new and published data, this led to 50-, 100-, and 150-yr intervals for selected time- series (Table 1). In order to distinguish between signals and noise, the equi-spaced "raw" data were first inspected by Singular Spectrum Analysis (SSA) (Vautard et al., 1992; Dettinger et al., 1995; Ghil et al., 2002), and the Mann-Kendall test was used to ascertain if there was a significant trend (95% significance level). These analyses were performed using the kspectra software package (kspectra, 2015). If a trend was identified (Table 1) it was extracted and the residuals from the trend were evaluated for significant cycles using the Maximum Entropy Method (MEM) (Kantz and Schrieber, 1997). The environmental trends (Fig. 4) show broad-scale multi-millennial changes. Constrained cluster analysis (Hammer et al., 2001) of the environmental and source (SSA1) standardized trend data, using Euclidean Distance as a measure of dissimilarity (Birks and Gordon, 1985) was used to detect major changes in data from 2322.

Previous Provenance and IRD Studies

Previous investigations of glacial marine sediment provenance in the Kangerlussuaq Trough (Fig. 2, part A) include radiogenic isotopes (Farmer et al., 2003; Dunhill, 2005; Simon, 2007; Verplanck et al., 2009; White et al., 2016) and qXRD of the <2 mm sediment (Andrews et al., 2015). The epsilon (Nd) and $^{87}Sr/^{86}Sr$ ratios all plot within the East Greenland/Iceland basalt provenance (Simon, 2007; Verplanck et al., 2009). White et al (2016) used $^{40}Ar/^{39}Ar$ and $^{206}Pb/^{204}Pb$ measurements on feldspars from a site within Kangerlussuaq Trough (KT) and a site seaward of core 2322 (PO175/GGC#7) (Alonso-Garcia et al., 2013) to show the dominance of sediments derived from erosion of the heavily glaciated flood basalts of the Geikie Plateau (Fig. 2, part A), but with some feldspars derived from the Caledonian Fold Belt to the north and the Nagssugtoqidian Mobile Belt to the west. In 2322 there is a steady decrease in the mafic (basalt-derived) fraction and an increase in the felsic fraction of the mineralogy through the Holocene (Andrews et al., 2015).

Studies of coarse >2 mm IRD along the Northeast/East Greenland shelf from over the past ca. 12,000 cal. yr B.P. documented a threefold division of the Holocene with early and late Holocene IRD contributions and a mid-Holocene interval of little to no coarse input (Andrews et al., 1997, 2014, 2016; Evans et al., 2002; Jennings et al., 2002b, 2006, 2011, 2013; Stein, 2008; Perner et al., 2016). This mid-Holocene thermal maximum interval was also a time when the Greenland Ice Sheet was behind its present-day margins.

There are presently no tidewater glaciers on Iceland and deposition of coarse IRD ceased ca. 10 cal ka B.P. (Castaneda et al., 2004). Studies of IRD around Iceland

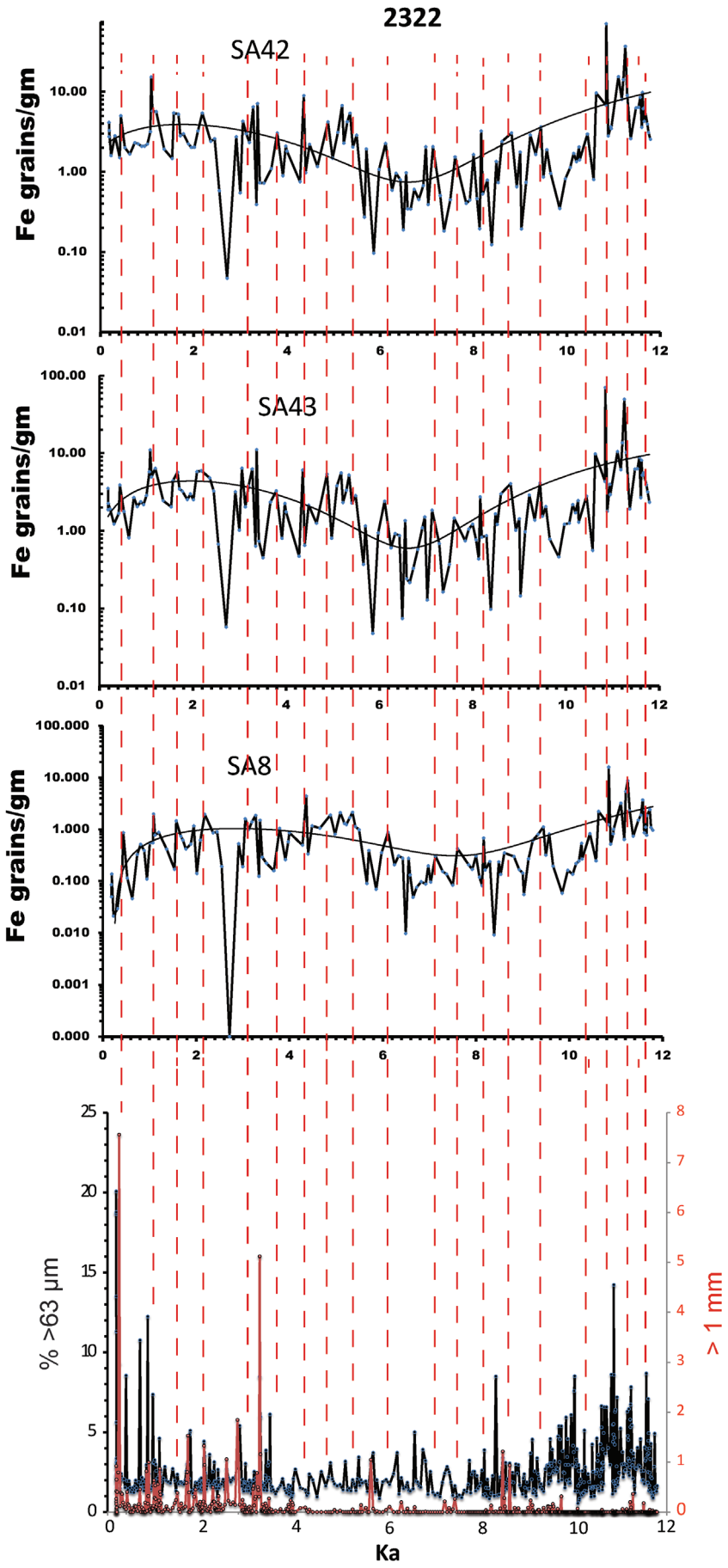

FIGURE 3. Fe grain numbers from core 2322 matched to East Greenland sources (42 and 43; see Fig. 1) as well as from the most important arctic source area, Banks Island (SA8). Note the approximately two- to sixfold increase in both the large East Greenland source areas from lows to highs. Greenland sources are in phase as are the arctic sources for nearly all peaks. The error of mismatch is one grain (1.5% of the total number matched, where this number is about 10–20 times the values shown because the average sample weight is 15 g). The polynomial fit for each shows a decrease in Fe grain matches in the mid-Holocene around 6–8 ka. This is also a low in coarse sediment. Red is >1 mm and black is >63 µm.

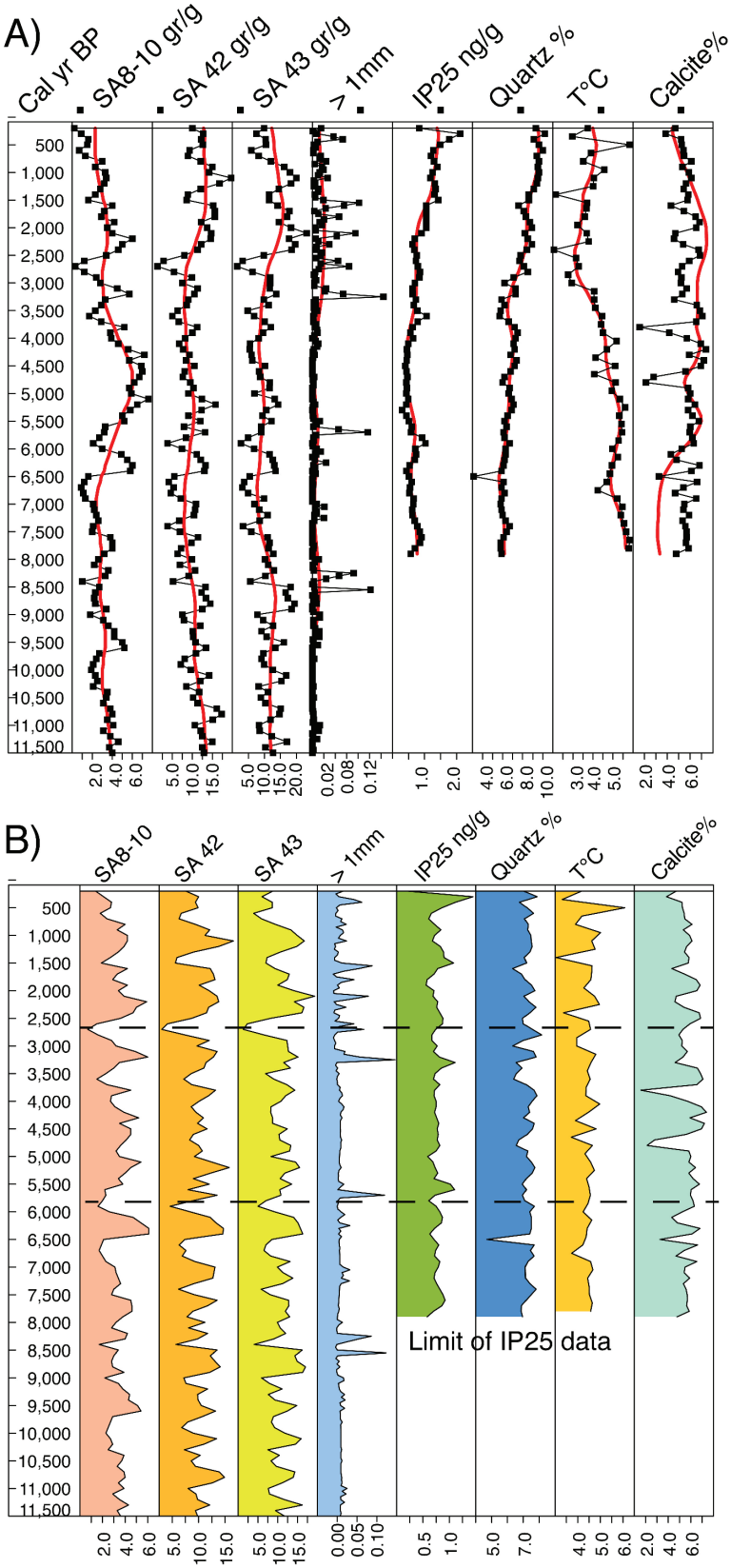

FIGURE 4. (A) Trends and integrated, equispaced data of the 100-yr equitime series of environmental parameters compared to those in the Fe grain matches to important source areas and IP_{25} values for core 2322. The Western Canadian Arctic (WCA), represents SA8-10 (Fig. 1). Red lines show the trends in the data, black lines are the original data. (B) Color panels show the detrended data (Table 1). Where no trend was detected (e.g., SA43) we plotted the reconstructed signal from the 1st SSA/PCA scores.

have focused on the presence of quartz as an indicator of ice rafting from non-Icelandic sources (Eiriksson et al., 2000; Andrews and Eberl, 2007; Andrews, 2009). The 100-yr regional reconstruction indicates a threefold history of quartz transport, and by inference the large-scale variations in drift ice (Andrews, 2009).

Results

We first present our data from Southeast Greenland, which provides multi-decadal evidence over the entire Holocene (shown in 2322 for the past 10–12 ka), and then consider the more detailed record from 2263 covering the past 2 cal ka B.P. from the Northwest Iceland Shelf across Denmark Strait from 2322 (Figs. 1 and 2, part A).

Core 2322

The Fe grain source data for this core are dominated by two primary source areas: SA42 and SA43 (Figs. 2, part A, and 3), and high grain counts from Arctic Ocean sites SA8-10, which include Banks Island (SA8) and sites further west, including the Mackenzie River (SA10), which we grouped into a single Western Canadian Arctic (WCA) estimate (Fig. 1). SA8 is by far the dominant source area in the WCA. The local source SA43 is dominant (average 31.0%), closely followed by the Northeast Greenland source SA42 (30.0%), and then by the combined Banks-Mackenzie area or WCA, SA8–10 (9.0%). There is only a small contribution from sediments linked to the Russian East Siberian Shelf and the Barents Sea Shelf edge, including Svalbard. The WCA source reflects the transport of sediment by sea ice during the Holocene (Darby, 2003). Of the total grains examined, 54% could not be attributed to a source within the current database.

In 2322, peaks of the ice-rafted Fe grains from SA42 and 43 are as high as 70 grains/g during the deglacial interval (10–12 ka) and as high as 15 grains/g during the younger parts (0–10 ka) of the Holocene (Fig. 3), with a mismatch in source error of less than one grain. There are nine circum-arctic sources that contributed Fe grains to core 2322. Of these nine sources, six contributed more than 3 Fe grains/g, and these regions are circled in red in Figure 1.

In Figure 4 we show the integrated, equi-spaced 100-yr time series, the trends, and the detrended data as determined from our analysis (kspectra, 2015). The environmental proxies in core 2322 have significant trends that explained between 15 and 82% of the variance (Table 1, and Fig. 4, part A). However, the trends in the Fe grain data from this core do not reach a statistically significant level. The SSA analysis indicated

TABLE 1

Sample resolution (spacing), trends, trend variance, and cycles for the studied cores.

	Proxies						Sources		
					Grain-size				
	IP_{25}	Qtz	T°C	Carbonate (%)	>1 mm	105–63 μm%	SA42	SA43	SA8
MD99-2322									
Sample spacing (yr)	100	100	150	100	50	50	100	100	100
Significant trend?	Yes	Yes	Yes	Yes	Yes	Yes	NO	NO	NO
Trend variance %	73	82	71	61	15	69			49
SSA1 variance %							33.6	32.7	45.4
MEM cycles (yr)							800	800	800
Strongest to weakest								400	400
(>0.95%)								485	340
								1070	1050
MD99-2633									
Sample spacing (yr)	50	50	50	50	100	NA	50	50	
Significant trend?	Yes	Yes	Yes	Yes	Yes		Yes	Yes	Insufficient
Trend variance %	78	58	83	78	90		81.3	55.7	grains
MEM cycles (yr)							240	350	
Strongest to weakest							300	250	
(>0.95%)							200	140	

that a large fraction (33 to 45%) of the variance in the signals was contained in the 1st Principal Component of each source series (Fig. 4, part A). Thus, although the environmental proxies all contained significant multi-millennial year trends, this is not reflected in the Fe grain sources. Indeed, the late Holocene increase in the sea ice biomarker and in quartz wt% is not reflected in the Fe grain data (Fig. 4, part A). However, the Fe grain data do show strong multi-century variability (Fig. 4, part B).

The environmental trends (Fig. 4, part A) show broad-scale multi-millennial changes. Constrained cluster analysis (Hammer et al., 2001) of the environmental and source standardized trend data for the past 8 cal ka B.P., using Euclidean Distance as a measure of dissimilarity (Birks and Gordon, 1985), indicated a major change occurred ca. 2.7 cal ka B.P. (Pangaea Data Publisher at https://doi.pangaea.de/10.1594/PANGAEA.876207) with secondary breaks at 5.5 and 1.45 cal ka B.P. These changes are consistent with the timing of paleoclimatic changes identified along the East/Northeast Greenland margin (Jennings et al., 2002b, 2011; Perner et al., 2015, 2016; Andrews et al., 2016).

To ascertain if there is any relationship between environmental variables and sources we standardized the data and ran an R-Mode Factor Analysis (Davis, 2002). Because of the differences in the sampling resolutions (Table 1), there are only 26 intervals (<8 cal ka B.P.) where data were available at the same time interval or core depth. The two Factor axes explained 72% of the variance, with the 1st axis showing that the trends on quartz wt%, carbonate %, the >1 mm sand, and IP_{25} were positively linked and, as might be expected, had a different sign from T°C, but also from the fine/medium sand fraction. Fe grains from SA42 and 43 also had strong positive loadings on the 1st PCA in contrast to the SA8 (or the WCA), which is only weakly associated with either PC1 or PC2 (Fig. 5), possibly because of the lower Fe grain numbers from that source area (Figs. 3 and 5).

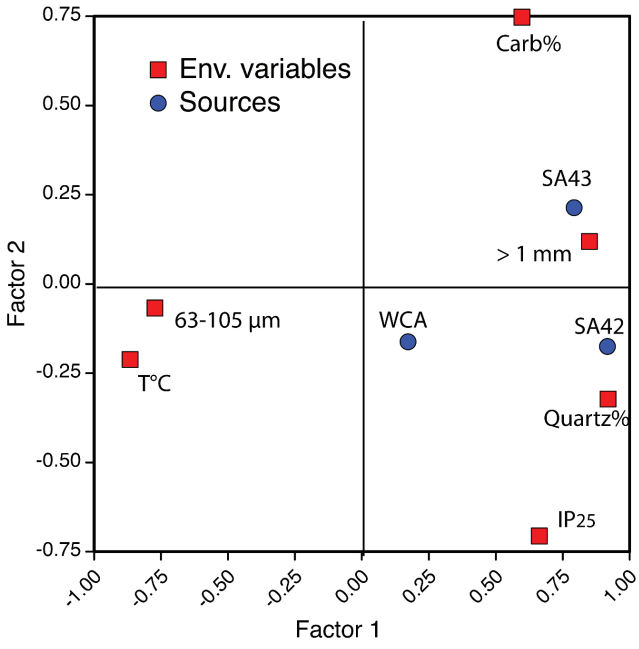

FIGURE 5. Bi-plot of the R-mode factor loadings for Fe grain sources and environmental proxies for 2322.

In detail, the trend data (Fig. 4, part A) show there is a steady increase in IP_{25} and quartz wt% over the past 4–5 cal kyr B.P., and this is also evident in records from the N Iceland Shelf (NIS) (cores 2263, MD99-2269, and JR51-GC35; Cabedo-Sanz et al., 2016). The most prominent feature of the IP_{25} profile in 2322, however, is a sharp increase during the past ca. 2 kyr and especially after ca. 1 ka B.P. (Figs. 4 and 6), both of which have counterparts in the NIS cores, and are interpreted in terms of enhanced drift ice delivery to both sides of Denmark Strait after ca. 2 ka. However, in contrast to the NIS cores, where IP_{25} and quartz wt% were well correlated (r^2 = 0.74 and 0.66 for MD99-2269 and JR51-GC35, respectively [Cabedo-Sanz et al., 2016]), their relationship is weaker for 2322 (r^2 = 0.44), likely indicating a change in provenance in one, or both, of the drift ice proxies. It is worth noting that the carbonate records in 2322 and MD99-2269 are virtually identical (Stoner et al., 2007). In contrast to the quartz and IP_{25} data, the Fe grain inputs from SA42 and 43 decreased slightly over the last 1400 cal. yr B.P., but remain above average for the Holocene (Fig. 3). This may reflect the effect of pervasive landfast sea ice restricting the passage of icebergs onto the shelf (Reeh et al., 2001; Reeh, 2004). There is widespread evidence across the northwestern Nordic Seas for a threefold division of the Holocene, although the timing of the transitions varies (Jennings et al., 2011; Müller et al., 2012; Perner et al., 2015; Cabedo-Sanz et al., 2016; Kristjansdóttir et al., 2016). The SSA trends on the SA42 and 43 Fe grain data from 2322 show a pronounced minimum at ca. 7 cal ka B.P. (Fig. 4, part A; Supplemental Data). This change at 6–8 ka is seen as a decrease in Fe grain numbers from all three dominant sources (SA42, 43, and 8; Fig. 3) and lends further credence to this threefold Holocene ice-rafting history.

The data in 2322 were biased by the very large amount of IRD and Fe grains in the deglacial interval (10–12 ka), so we truncated the data set at 10 ka before running the time series analysis. The MEM 100-yr spacing time series shows that there is a dominant ~800-yr cycle in all three sources (>0.95 confidence

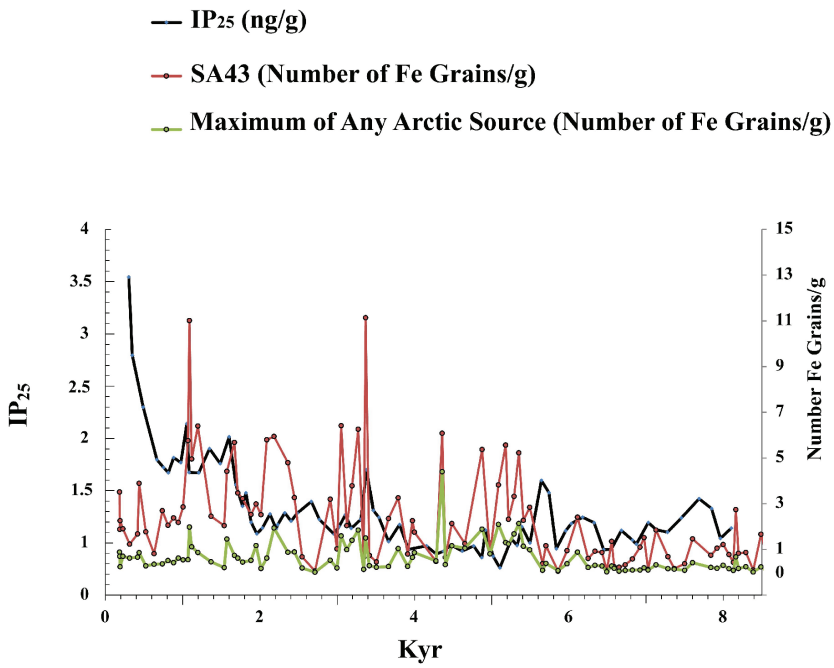

FIGURE 6. Plot of the IP_{25} and Fe grain data in 2322 with their original (not 100-yr integrated) values showing the sharp increase in IP_{25} over the last millennium, but the slight decrease in Southeast Greenland source SA43.

level) (Fig. 7). There is also a significant 400-yr cycle in SA42 and SA8-10.

Core 2263

The grain-size spectra in this core are described as "muddy sands," with median grain size varying between 48 and 103 μm (Blott and Pye, 2001). The median diameter decreased steadily over the past 2 cal ka B.P. with a relatively abrupt shift to finer-grained sediments at ca. 900 cal. yr B.P., which is also matched by the decrease in the calcite wt% (Fig. 8, part A). There is no characteristic coarse IRD shoulder on the spectra, which is a common feature of sites with major iceberg sediment input, such as sites in Nansen Trough (Prins et al., 2002; Perner et al., 2016). The matched grain counts are higher at this site than in the more proximal 2322 site, probably because of the winnowing of the sediment by strong bottom currents (Thors, 1974; Ólafsdóttir, 2004).

The presence of Fe grains matched specifically to East Greenland source areas (SA42 and 43) as well as several Arctic Ocean source areas found in this core indicate that IRD from all of these sources reached this core site throughout the Holocene (Fig. 8, part A). Of the total grains examined, 41% could not be attributed to a source within the current database. The association between several environmental proxies was discussed by Axford et al. (2011), who showed that IP_{25} and quartz weight percent were inversely correlated with water T°C estimates. We computed the trends and residuals from the trends for environmental parameters (Fig. 8, part A, Table 1) and compared those with the trend data from the major source areas as determined from the Fe grain data (Figs. 8, part A, and 9, part A). All data were recalculated to 50-yr time-steps (Fig. 8). Calcite weight percent is included as a measure of marine productivity because the surface freshwater cap that limits mixing and nutrient replenishment inversely influences it (Thordardóttir, 1984, 1986; Andrews et al., 2001). Analysis of the time series (Table 1, Fig. 8, part A) indicates that there is a significant trend in the 1st SSA axis that explains between 48 and 90% of the variance. The five environmental proxies indicate that over the past 750 yrs, that is from the onset of the Little Ice Age (LIA; A.D. ca. 1300–1850) (Miller et al., 2012), temperatures, calcite wt%, and median grain size decreased, whereas quartz and IP_{25} increased. Both quartz and IP_{25} have a noticeable increase beginning ca 600–700 yr B.P. coinciding with local and regional evidence for the onset of the LIA (Geirsdóttir et al., 2009; Jónsdóttir et al., 2015), perhaps driven by an interval of volcanism and an increase in sea ice across the North Iceland shelf, more generally (Massé et al., 2008; Miller et al., 2012; Cabedo-Sanz et al., 2016). Residuals from the trends (Fig. 8, part B) show no obvious correlations.

The 50-yr integrated Fe grain data show significant trends for both Greenland Fe grain sources that explain 81 and 56% of the variance in the series (Table 1, Fig. 8, part A). They indicate an overall decrease over the record, and this contrasts with the increase in IP_{25} and quartz wt% (Fig. 8, part A), which have been linked to the regional LIA (Andrews et al., 2009a). The dominant

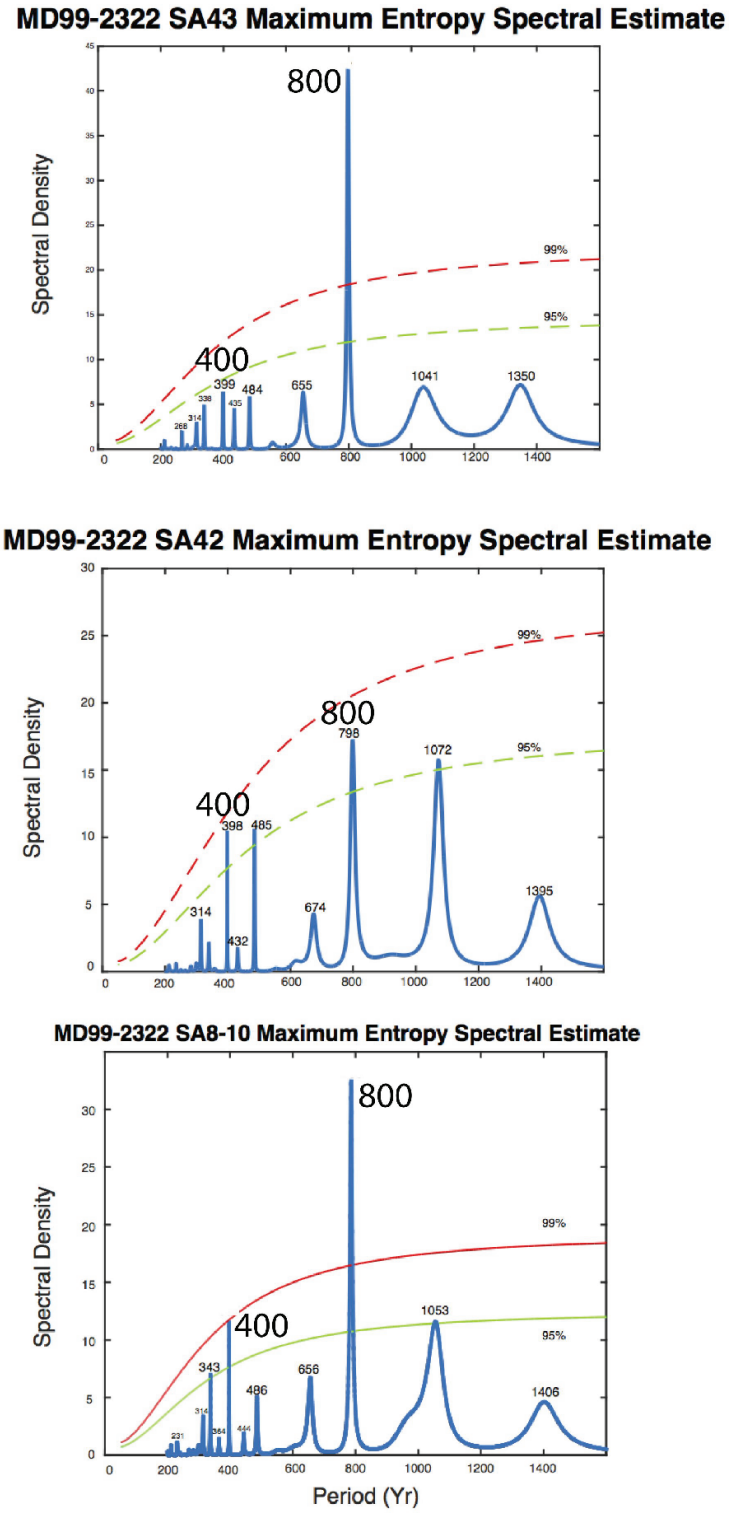

FIGURE 7. Time series analyses using MEM for the Holocene record of Fe grain matches to important sources from Greenland (SA42 and 43) and the Arctic Ocean, Western Canadian Arctic (SA8-10) in core 2322.

Arctic Ocean source for Fe grains in 2263 is SA8 (Banks Island, CAA, Fig. 1), but there are significant contributions from SA30-32, the Svalbard archipelago (Fig. 1). The trends on the SA8 and SA30-32 (not shown) have an overall increase toward the present, similar to the trends for quartz wt% and IP_{25}, but not as pronounced (Fig. 8, part A). In both these arctic regions IP_{25} has been shown as a reliable proxy for sea ice (Belt et al., 2007, 2013, 2015; Brown et al., 2011; Müller et al., 2011; Xiao et al., 2015), and our data might suggest an increased transport from these areas during the LIA (Figs. 8 and 9). These Arctic Ocean trends contrast with those from East Greenland sources, SA42 and 43, which have decreased over the past few centuries (Figs. 8, part A, and

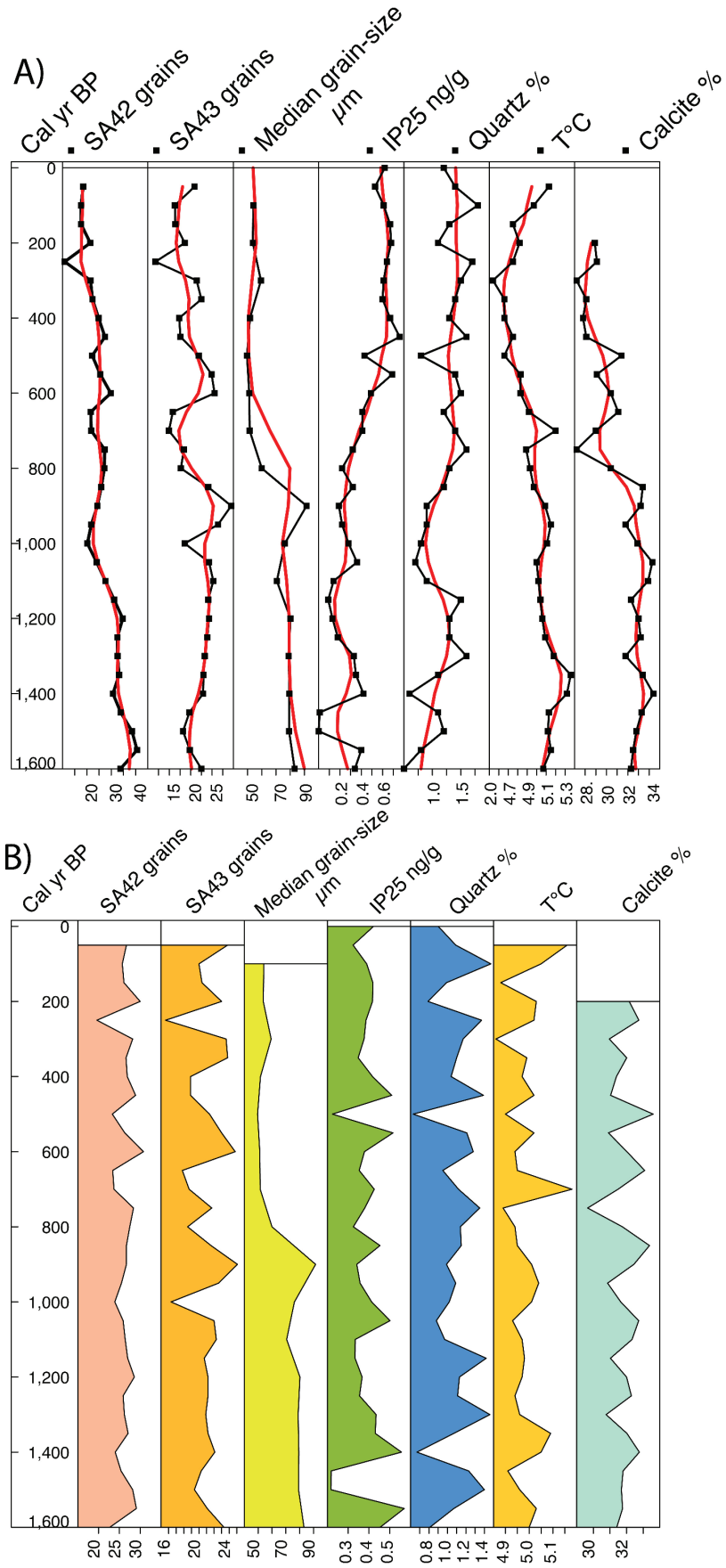

FIGURE 8. (A) Trends and matched data (Fe grains) of the 50-yr time series and environmental proxies (Table 1) for matches to important source areas. Red lines indicate the trends in the data, black lines show the integrated data. (B) Color panels show the residuals from the trends depicted in part A.

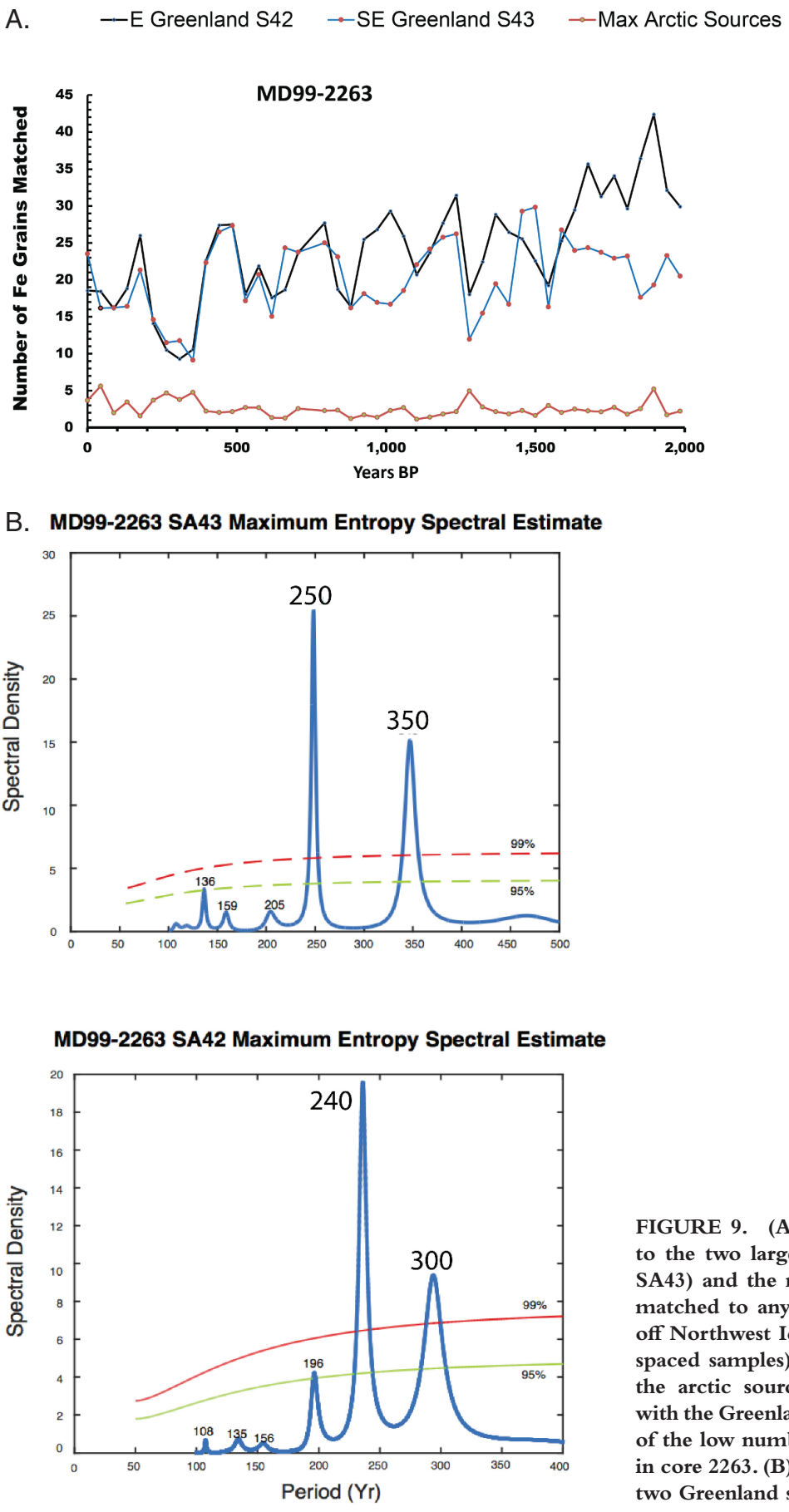

FIGURE 9. (A) Number of Fe grain matches to the two large Greenland sources (SA42 and SA43) and the maximum number of Fe grains matched to any one arctic source in core 2263 off Northwest Iceland (not integrated to evenly spaced samples). Note that unlike in core 2322, the arctic sources do not vary synchronously with the Greenland source.This could be because of the low number of Fe grains from the Arctic in core 2263. (B) MEM spectral estimates for the two Greenland sources for 2263.

9, part A). Residuals from the trends (Fig. 8, part B) for both the SA42 and 43 Fe grain sources show significant cycles (Fig. 9, part B).

Discussion

Until now, the application of Fe grain source identification has been restricted to cores from the Arctic Basin (Darby and Bischof, 2004; Darby and Zimmerman, 2008; Darby et al., 2012) with the exception of one study from North Iceland (Andrews et al., 2009b) and one from East Greenland (Alonso-Garcia et al., 2013). Hence, the focus of ice-rafted sediments has been associated with sea ice. In our study, especially given the location of 2322 (Fig. 2, part A) and the records of coarse IRD input associated with icebergs (Andrews et al., 1997; Jennings et al., 2011; Perner et al., 2016), we must also consider inputs from turbid meltwater plumes (Syvitski et al., 1996; Smith and Andrews, 2000) and sediment reworking from iceberg scouring (Syvitski et al., 2001) and bottom currents. Some 5000 km^3 of sea ice is exported through Fram Strait per year (Hebbeln and Wefer, 1991), whereas the volume of icebergs produced per year from Northeast/East Greenland is two orders of magnitude smaller (Bigg, 1999). However, only an estimated 5% of the arctic sea ice contains sediment, and this portion carries smaller concentrations than most icebergs (Darby, 2003; Darby et al., 2011), although icebergs calved into the fjords lose significant and varying sediment content through melting before they reach the shelf (e.g. Stein et al., 1993; Syvitski et al., 1996). The coastal waters off East Greenland are too deep to facilitate the processes associated with entrainment of sediment into sea ice seen on the shallow arctic shelves (Reimnitz et al., 1992, 1993; Darby, 2003; Dethleff, 2005; Dethleff and Kuhlmann, 2009). Sediment shed onto the land-fast ice is the result of fjord wall slope failures and is generally very coarse (Gilbert, 1990), unlike the sediment in 2322. Also, our Fe grain proxy has a median size of 100 μm, which is much coarser than the median size of sediment in core 2322. This anomaly is more typical of ice-rafted grains than any other transport mode or reworking of sediment.

As noted earlier, interpretation of changes in IRD can be attributed to changes in sediment entrainment at the source, the volume of transport in either icebergs or sea ice, and changes in oceanography, especially changes in the temperature of surface or (in the case of icebergs) intermediate waters that affect melting. We should also note that the absence of IRD and IP_{25}, could both be because of (1) open water, no icebergs or sea ice, or (2) pervasive land-fast sea ice, which restricts the movement of icebergs (Dwyer, 1995; Reeh et al., 2001) and limits IP_{25} production (Belt and Müller, 2013).

Driftwood is exported on sea ice through Fram Strait from the Russian and North American shelves and is beached on the North and East Greenland coasts (Funder et al., 2011; Hellmann et al., 2015). We would thus predict that sediments with an arctic shelf provenance (Fig. 1) would be present in 2322, although possibly overwhelmed by locally derived glacial sediments. Despite the Russian driftwood evidence, the number of sand-size Fe grains from the Siberian shelf where this driftwood originates is small, possibly because of the fine-grained nature of East Siberian Shelf source sediments (Wahsner et al., 1999). There are no detailed data on the grain-size distributions for 2322 but information is available on several fractions <1 mm. On a nearby core JM96-1214GC in the Kangerlussuaq inner basin (Jennings et al., 2002a), the Holocene sediments are described as medium to very fine silts. Given the small weight percentages of grains >1 mm and 63–105 μm (Figs. 3 and 4), the 2322 sediments are also dominantly silts and clays. Even cores close to the coast and clearly subject to iceberg rafting are generally dominated by silt with limited sand (Perner et al., 2016). The sea ice biomarker IP_{25} was present in all sediment horizons, consistent with continuous drift ice delivery to the site after 8 ka.

Given the fine-grained nature of the sediment from SA42 and 43, and the absence of coarse sand, contributions in 2322 from these source areas may reflect transport as suspended sediment plumes, fine-grained glacial and subglacial sediments entrained in icebergs, or fine sediments resuspended by iceberg scouring of the adjacent shallower banks. The fact that Fe grains are coarser, and the median size much coarser, than the sediment in 2322, argues that these grains are ice-rafted.

Both cores have similar numbers of Fe grains from SA43 (Figs. 3 and 8, part A; Pangaea archived data) despite the proximity of SA43 to core 2322 (Fig. 2, part A). The average increase from trough to peak for SA42 and 43 is 10 and 12 Fe grains, respectively, in cores 2322 and 2263. Even SA46, located immediately north of SA42 (Figs. 1 and 2, part A), contributed statistically significant numbers of Fe grains to core 2322. The fact that SA42 is so high in core 2322 would argue that iceberg rafting has to be the dominant mode of IRD delivery and not sediment plumes or reworking from local sources. Obviously any input from local sediment plumes or reworking does not swamp the more distal sources that must be ice-rafted.

The presence of abundant Siberian driftwood on Iceland beaches as well as the Fe grains from arctic shelf sources in core 2263 unequivocally demonstrates that

drift ice from the arctic shelf reaches Iceland (Eggertsson, 1993; Hellmann et al., 2015), a conclusion corroborated by the occurrence of IP_{25} in various surface sediments from the North Iceland shelf (Cabedo-Sanz et al., 2016). However, driftwood occurrence provides no information on the contribution from Greenland drift ice, mainly in the form of icebergs (Koch, 1945), so we look to Fe grain geochemical data to provide information on the contributions from Greenland as well as the arctic margins (Darby et al., 2015). At both core sites we expect delivery of sediment entrained in icebergs and/or sea ice. We expect that the amount of IRD contained on, or in, East/North Greenland sea ice to be small and primarily restricted to delivery of sediment from fjord walls during the spring melt. In both 2263 and 2322, the Fe grains increase and decrease synchronously between the East Greenland sources (SA42, and 43) but the prominent arctic source (SA8) is synchronous with the Greenland sources only in core 2322; it occurs in too low abundance in core 2263 to evaluate its synchronicity (Figs. 3 and 8, part A). Fe grains in 2322 are in approximate agreement with increases in the coarse IRD fraction (Fig. 3), although this is not the case in 2263 (Fig. 9, part A). In 2322 the plot of the Fe grain matches to the two most important sources, East/Northeast Greenland (SA42) and Southeast Greenland (SA43), show cyclic changes throughout the last 10 cal ka (Figs. 3 and 7) with a long-term trend showing a decrease during the middle Holocene (Fig. 3). The same cycles are seen in the SA8 arctic Fe grain input to 2322.

This shared cyclicity for IRD input from such a wide area suggests that the export of sea ice from the Arctic Ocean is also cyclic and in synchronization with the East Greenland iceberg production or iceberg melting, or that the cyclicity is governed by one or more of the following: (1) oceanic influences such as the release of siqussaq, (2) changes in the land-fast ice distribution, and/or (3) enhanced drift ice melting at the polar front. The MEM analysis of the detrended data indicate that two cycles for both source areas (SA42 and SA43) between 236 and 248 yrs and between 294 and 348 yrs in core 2263 are significant at 0.99 probability (Fig. 9, part B). A 196-yr cycle, significant at 0.95 for SA42 (Fig. 9, part B), is similar to the 205-yr de Vries total solar intensity (TSI) cycle (Wagner et al., 2001; Darby et al., 2012). Further studies are needed to confirm this relationship as the cycles are off by a few years between Fe grain sources and TSI, possibly due to errors in the age model for 2263. However, if a ca. 200-yr Fe grain cycle from SA42 is found in future studies, it could help explain the nature of the Fe grain cycles in 2263 as being because of feedbacks from this weak solar intensity increase to melting or iceberg production from this source in Greenland. Note that different conclusions for the statistical significance of the data are reached vis-a-vis the Run Test versus the MEM (Figs. 4, part B, and 7). These differences are probably associated with the different underlying null hypotheses as the Run Test examines variations about the mean and does not take into account "turning points" (Miller and Kahn, 1962).

There is also a significant 400-yr cycle (>0.95) that could be related to the 800-yr cycle where the 800-yr cycle may be a multiple of the 400-yr cycle. This 400-yr cycle is seen in other records and attributed to TSI (Neff et al., 2001; Domack et al., 2001; Strikis et al., 2011; Bugelmayer-Blaschek et al., 2016). Like the 205-yr de Vries TSI cycle seen in 2263, this 800-yr cycle in 2322 suggests that changes in solar intensity might be a factor in driving these Fe grain and IRD cycles. The cycles for the Greenland sources are also in phase, peaking at the same times in both cores (Figs. 3 and 8, part A). Because the Arctic Oscillation 1550-yr cycle (Darby et al., 2012) is an approximate multiple of this 800-yr cycle, there is a suggestion that atmospheric change might impact the IRD delivery at 2322.

These results compare with cycles of drift ice proxies IP_{25} and quartz in a core on the North Iceland shelf (core MD99-2269, Cabedo-Sanz et al., 2016) indicating the presence of drift ice carried by the East Iceland Current. Time series on these two proxies show significant cycles close to 200 yrs (213 and 208, respectively, Cabedo-Sanz et al., 2016). Other cycles for these two proxies in MD99-2269 occur at 1024, 275, 334, and 156 yrs. Slight differences with the cycles from core 2322 and MD99-2269 are unlikely to be due to errors in the age models for these cores because these two cores share a chronology based on depth correlation of the paleomagnetic secular variation (Stoner et al., 2007).

This Fe grain data set marks the farthest south occurrence of definitive IRD from the Arctic Ocean, although Russian and Canadian driftwood have been found even farther south. But driftwood could drift for at least a year after it is released from ice. The fluctuations of the circum-arctic Fe grains, which are sea ice rafted are in phase with those from Greenland, which are iceberg rafted (Fig. 3), suggesting a common link between sea ice and iceberg IRD.

The abundance of Fe grains from SA43 in core 2263 is somewhat surprising given the prominent circulation patterns in this area (Fig. 1). This source in 2263 most likely comes from the Scoresby Sund area of SA43 (Fig. 2, part A). Maps of iceberg distributions affecting Icelandic waters (Iceland Meteorological Office, 1987, 1988) indicate that the major source areas for icebergs are Scoresby Sund and further north along the Northeast Greenland coast. These icebergs might well reach core

2263 by adiabatic winds from the Greenland ice sheet or some other source of westerly winds that could move icebergs eastward to 2263.

Conclusions

This study, combining multiple proxies in two cores near Denmark Strait, clearly shows that arctic sea ice not only reaches this area but transports sediment from multiple areas around the arctic shelves nearly 1800 km south of the Arctic Ocean and up to more than 4000 km of total drift before melting and depositing this sediment. The use of precise and accurate source determination of Fe grains using 14 elements and trace elements in eight different Fe oxide minerals enables us to conclude not only that these Fe grains originate thousands of kilometers away in the Arctic Ocean but also that they are not randomly deposited in time. Both nearby Greenland sources and Arctic Ocean shelf sources occur in both cores at cyclic intervals of ~240 and 800 yrs in cores 2263 and 2322, respectively. The occurrence of Fe grains in 2322 off Southeast Greenland from two primary source areas on East and Southeast Greenland in synchronization with Fe grains from the arctic shelves suggests that some regional climatic forcing might be involved. Because the significant cycles in both cores correspond to total solar intensity cycles, the feedback from these weak solar fluctuations might be driving the melting and/or production of icebergs/sea ice in both Greenland and the Arctic Ocean.

The Arctic Oscillation (AO) is thought to influence ice export through Fram Strait (Rennermalm et al., 2007) and thus could be involved with the pulses of Fe grains and IRD from the Arctic seen in core 2322. The fact that the 1550-yr AO seen in a high resolution Holocene core off northern Alaska (Darby et al., 2012) is a multiple of the 800-yr cycle seen in Fe grain peaks from the Arctic Ocean raises the possibility that the AO is somehow influenced by solar intensity fluctuations. This premise was thought unlikely because there was no solar cycle at 1550 yrs (Darby et al., 2012). So whether the AO cyclicity is forced by internal variability in the climate system or fluctuations in solar intensity is still open to investigation.

Acknowledgments

The research of Darby, Andrews, and Jennings was supported by grant ANS-1107761 from the National Science Foundation. Cores 2263 and 2322 were also obtained with funding from NS –OCE-9807761. We thank R. Stein and an anonymous reviewer for their helpful suggestions. The work of Belt, Cabedo-Sanz, and Jennings was also supported by their involvement in the ANATILS project (Abrupt North Atlantic Transitions: Ice, Lakes and Sea) supported by the Icelandic Research Council (RANNIS) Grant of Excellence #141573-051 awarded to Á. Geirsdóttir (University of Iceland) and G. Miller (INSTAAR) as PIs. We also thank the staff at the Oregon State University Marine Geology Repository for sampling core MD99-2269 and -2322 (grant number OCE-0962077), and INSTAAR's participation in the two legs of the IMAGES V Cruise that obtained cores 2263 and 2322 was supported by NSF-OCE-980900. The Fe grain data used in this study are deposited in the Pangaea Data Publisher (http://www.Pangaea.de).

References Cited

Aitchison, J., 1986: *The Statistical Analysis of Compositional Data*. London: Chapman and Hall, 416 pp.

Alonso-Garcia, M., Andrews, J. T., Belt, S. T., Cabedo-Sanz, P., Darby, D., and Jaeger, J., 2013: A multi-proxy and multi-decadal record (to AD 1850) of environmental conditions on the East Greenland shelf (~66°N). *The Holocene*, 23: 1672–1683.

Amundson, J. M., Fahnestock, M., Truffer, M., Brown, J., Luthi, M. P., and Motyka, R. J., 2010: Ice mélange dynamics and implications for terminus stability, Jakobshavn Isbræ, Greenland. *Journal of Geophysical Research–Earth Surface*, 115: *F01005, doi: http://dx.doi.org*/10.1029/2009JF001405.

Andrews, J. T., 2000: Icebergs and Iceberg Rafted Detritus (IRD) in the North Atlantic: facts and assumptions. *Oceanography*, 13: 100–108.

Andrews, J. T., 2009: Seeking a Holocene drift ice proxy: non-clay mineral variations from the SW to N-central Iceland shelf: trends, regime shifts, and periodicities. *Journal of Quaternary Science*, 24: 664–676.

Andrews, J. T., and Eberl, D. D., 2007: Quantitative mineralogy of surface sediments on the Iceland shelf, and application to down-core studies of Holocene ice-rafted sediments. *Journal of Sedimentary Research*, 77: 469–479.

Andrews, J. T., and Jennings, A. E., 2014: Multidecadal to millennial marine climate oscillations across the Denmark Strait (~66°N) over the last 2000 cal yr BP. *Climate of the Past*, 10: 325–343.

Andrews, J. T., and Vogt, C., 2014a: Results of bulk sediment X-ray diffraction analysis and quantification of mineral phases based on the RockJock and on the QUAX quantitative analysis. *Pangaea*, https://doi.pangaea.de/10.1594/PANGAEA.830397.

Andrews, J. T., and Vogt, C., 2014b: Source to sink: statistical identification of regional variations in the mineralogy of surface sediments in the western Nordic Seas (58°N–75°N; 10°W–40°W). *Marine Geology*, 357: 151–162.

Andrews, J. T., Milliman, J. D., Jennings, A. E., Rynes, N., and Dwyer, J., 1994: Sediment thicknesses and Holocene glacial

marine sedimentation rates in three East Greenland fjords (ca. 68°N). *Journal of Geology*, 102: 669–683.

Andrews, J. T., Smith, L. M., Preston, R., Cooper, T., and Jennings, A. E., 1997: Spatial and temporal patterns of iceberg rafting (IRD) along the East Greenland margin, ca. 68°N, over the last 14 cal.ka. *Journal of Quaternary Science*, 12: 1–13.

Andrews, J. T., Helgad**ó**ttir, G., Geirsd**ó**ttir, A., and Jennings, A. E., 2001: Multicentury-scale records of carbonate (hydrographic?) variability on the N. Iceland margin over the last 5000 yrs. *Quaternary Research*, 56: 199–206.

Andrews, J. T., Belt, S. T., **Ólafsdóttir**, S., Masse, G., and Vare, L., 2009a: Sea ice and marine climate variability for NW Iceland/Denmark Strait over the last 2000 cal. yr BP. *The Holocene*, 19: 775–784.

Andrews, J. T., Darby, D. A., Eberl, D. D., Jennings, A. E., Moros, M., and Ogilvie, A., 2009b: A robust multi-site Holocene history of drift ice off northern Iceland: implications for North Atlantic climate. *The Holocene*, 19: 71–78.

Andrews, J. T., Jennings, A. E., Coleman, C. G., and Eberl, D., 2010: Holocene variations in mineral and grain-size composition along the East Greenland glaciated margin (ca 67–70°N): local versus long-distant sediment transport. *Quaternary Science Reviews*, 29: 2619–2632.

Andrews, J. T., Bigg, G. R., and Wilton, D. J., 2014: Holocene sediment transport from the glaciated margin of East/Northeast Greenland (67–80°N) to the N Iceland shelves: detecting and modeling changing sediment sources. *Quaternary Science Reviews*, 91: 204–217.

Andrews, J. T., Bjork, A. A., Eberl, D. D., Jennings, A. E., and Verplanck, E. P., 2015: Significant differences in late Quaternary bedrock erosion and transportation: East versus West Greenland ~ 70°N and the evolution of glacial landscapes. *Journal of Quaternary Science*, 30: 452–463.

Andrews, J. T., Stein, R., Moros, M., and Perner, K., 2016: Late Quaternary changes in sediment composition in NE Greenland fjords, shelf, slope, and deep sea. *Boreas*, 45(3): 381–397, doi: http://dx.doi.org/10.1111/bor.12169.

Arndt, J. E., Jokat, W., and Dorschel, B, 2017: The last glaciation and deglaciation of the Northeast Greenland continental shelf revealed by hydro-acoustic data. *Quaternary Science Reviews*, 160: 45–56.

Axford, Y., Andresen, C., Andrews, J. T., Belt, S. T., Geirsd**ó**ttir, A., Masse, G., Miller, G. H., **Ólafsdóttir**, S., and Vare, L. L., 2011: Do paleoclimate proxies agree? Statistical comparison of climate and sea-ice reconstructions from Icelandic marine and lake sediments, 300–1900 AD. *Journal of Quaternary Science*, 26: 645–656.

Belt, S. T., and Müller, J., 2013: The Arctic sea ice biomarker IP_{25}: a review of current understanding, recommendations for future research and applications in palaeo sea ice reconstructions. *Quaternary Science Reviews*, 79: 9–25.

Belt, S. T., Massé, G., Rowland, S. J., Poulin, M., Michel, C., and LeBlanc, B., 2007: A novel chemical fossil of palaeo sea ice: IP_{25}. *Organic Geochemistry*, 38: 16–27.

Belt, S. T., Brown, T. A., Ringrose, A. E., Cabedo-Sanz, P., Mundy, C. J., Gosselin, M., and Poulin, M., 2013: Quantitative measurement of the sea ice diatom biomarker IP_{25} and sterols in Arctic sea ice and underlying sediments: further considerations for palaeo sea ice reconstruction. *Organic Geochemistry*, 62: 33–45.

Belt, S. T., Cabedo-Sanz, P., Smik, L., Navarro-Rodriguez, A., Berben, S. M., Knies, J., and Husum, K., 2015: Identification of paleo Arctic winter sea ice limits and the marginal ice zone: optimised biomarker-based reconstructions of late Quaternary Arctic sea ice. *Earth and Planetary Science Letters*, 431: 127–139.

Bigg, G. R., 1999: An estimate of the flux of iceberg calving from Greenland. *Arctic, Antarctic, and Alpine Research*, 31: 174–178.

Birks, H. J. B., and Gordon, A. D., 1985: *Numerical Methods in Quaternary Pollen Analysis*. London: Academic Press Inc., 317 pp.

Blott, S. J., and Pye, K., 2001: GRADISTAT: a grain size distribution and statistics package for the analysis of unconsolidated sediments. *Earth Surface Processes and Landforms*, 26: 1237–1248.

Brooks, C. K., 1990: Kangerdlugssuaq Studies: Processes at a Rifted Continental Margin, Conference Proceedings. Geological Institute, University of Copenhagen, Copenhagen, Denmark, 100 pp.

Brooks, C. K., 2008: A new geological map of East Greenland. *Geology Today*, 24: 28–30.

Brown, T. A., Belt, S. T., Philippe, B., Mundy, C. J., Massé, G., Poulin, M., and Gosselin, M., 2011: Temporal and vertical variations of lipid biomarkers during a bottom ice diatom bloom in the Canadian Beaufort Sea: further evidence for the use of the IP_{25} biomarker as a proxy for spring Arctic sea ice. *Polar Biology*, 34: 1857–1868.

Bugelmayer-Blaschek, M., Roche, D. M., Renssen, H., and Andrews, J. T., 2016: Internal ice-sheet variability as source for the multi-century and millennial-scale iceberg events during the Holocene? A model study. *Quaternary Science Reviews*, 138: 119–130.

Cabedo-Sanz, P., Belt, S. T., Jennings, A. E., Andrews, J. T., and Geirsd**ó**ttir, A., 2016: Variability in drift ice export from the Arctic Ocean to the North Icelandic Shelf over the last 8,000 years: a multi-proxy evaluation. *Quaternary Science Reviews*, 146: 99–115.

Castaneda, I. S., Smith, M. L., Kristjansd**ó**ttir, G. B., and Andrews, J. T., 2004: Temporal changes in Holocene $\delta^{18}O$ records from the northwest and central North Iceland Shelf. *Journal of Quaternary Science*, 19: 1–14.

Clark, P. U., and Pisias, N. G., 2000: Interpreting iceberg deposits in the deep sea. *Science*, 290(5489): 51-52.

Darby, D. A., 2003: Sources of sediment found in the sea ice from the western Arctic Ocean, new insights into processes of entrainment and drift patterns. *Journal of Geophysical Research*, 108(C8): 3257, doi: http://dx.doi.org/10.1029/2002JC001350.

Darby, D. A., and Bischof, J. F., 1996: A statistical approach to source determination of lithic and Fe-oxide grains: an example from the Alpha Ridge, Arctic Ocean. *Journal of Sedimentary Research*, 66(3): 599–607.

Darby, D. A., and Bischof, J., 2004: A Holocene record of changing Arctic Ocean ice drift analogous to the effects of the Arctic Oscillation. *Palaeoceanography*, 19: PA1027, doi: http://dx.doi.org/10.1029/2003PA000961.

Darby, D. A., and Zimmerman, P., 2008: Ice-rafted detritus events in the Artic during the last glacial interval, and the timing of the Innuitian and Laurentide ice sheet calving events. *Polar Research*, 27: 114–127.

Darby, D. A., Myers, W. B., Jakobsson, M., and Rigor, I., 2011: Modern dirty sea ice characteristics and sources: the role of anchor ice. *Journal of Geophysical Research–Oceans*, 116: 1978–2012.

Darby, D. A., Ortiz, J. D., Grosch, C. E., and Lund, S. P., 2012: 1,500-year cycle in the Arctic Oscillation identified in Holocene Arctic sea-ice drift. *Nature Geoscience*, 5: 897–900.

Darby, D. A., Myers, W., Herman, S., and Nicholson, B., 2015: Chemical fingerprinting, a precise and efficient method to determine sediment sources. *Journal of Sedimentary Research*, 85: 247–253.

Davis, J. C., 2002: *Statistics and Data Analysis in Geology*. 3rd edition. New York: John Wiley and Sons, 656 pp.

Dethleff, D., 2005: Entrainment and export of Laptev Sea ice sediments, Siberian Arctic. *Journal of Geophysical Research–Oceans*, 110: C07009, doi: http://dx.doi.org/10.1029/2004JC002740.

Dethleff, D., and Kuhlmann, G., 2009: Entrainment of fine-grained surface deposits into new ice in the southwestern Kara Sea, Siberian Arctic. *Continental Shelf Research*, 29: 691–701.

Dettinger, M. D., Ghil, M., Strong, C. M., Weibel, W., and Yiou, P., 1995: Software expedites singular-spectrum analysis of noisy time series. *EOS, Transactions of the American Geophysical Union*, 76(2): 12–21.

Divine, D. V., and Dick, C., 2006: Historical variability of the sea ice edge position in the Nordic Seas. *Journal of Geophysical Research*, 111(C1): 14 pp., doi: http://dx.doi.org/10.1029/2004JC002851.

Domack, E., Leventer, A., Dunbar, R., Taylor, F., Brachfeld, S., Sjunneskog, C., and ODP Leg 178 Scientific Party, 2001: Chronology of the Palmer Deep site, Antarctic Peninsula: a Holocene palaeoenvironmental reference for the circum-Antarctic. *The Holocene*, 11: 1–9.

Dunhill, G., 2005: Iceland and Greenland margins: a comparison of depositional processes under different glaciological and oceanographic settings, Ph.D. thesis, Department of Geological Sciences, University of Colorado, Boulder, 242 pp.

Dwyer, J. L., 1995: Mapping tide-water glacier dynamics in East Greenland using Landsat data. *Journal of Glaciology*, 41: 584–596.

Eggertsson, O., 1993: Origin of the driftwood on the coasts of Iceland: a dendrochronological study. *Jokull*, 43: 15–32.

Eiriksson, J., Knudsen, K. L., Haflidason, H., and Henriksen, P., 2000: Late-glacial and Holocene paleoceanography of the North Iceland Shelf. *Journal of Quaternary Science*, 15: 23–42.

Evans, J., Dowdeswell, J. A., Grobe, H., Niessen, F., Stein, R., Hubberten, H.-W., and Whittington, R. J., 2002: Late Quaternary sedimentation in Kejser Joseph Fjord and the continental margin of East Greenland. *In* Dowdeswell, J. A., and Cofaigh, C. Ó. (eds.), *Glacier-Influenced Sedimentation on High-Latitude Continental Margins*. Geological Society, London, Special Publications, 203: 149–179.

Farmer, G. L., Barber, D. C., and Andrews, J. T., 2003: Provenance of Late Quaternary ice-proximal sediments in the North Atlantic: Nd, Sr and Pd isotopic evidence. *Earth and Planetary Science Letters*, 209: 227–243.

Funder, S., Goosse, H., Jepsen, H., Kaas, E., Kjaer, K. H., Korsgaard, N. J., Larsen, N. K., Linderson, H., Lysa, A., Moller, P., Olsen, J., and Willerslev, E., 2011: A 10,000-year record of Arctic Ocean sea-ice variability—View from the beach. *Science*, 333(6043): 747–750.

Geirsd**ó**ttir, A., Andrews, J. T., **Ólafsdóttir**, S., Helgad**ó**ttir, G., and Hardard**ó**ttir, J., 2002: A 36 ka record of iceberg rafting and sedimentation from north-west Iceland. *Polar Research*, 21: 291–298.

Geirsd**ó**ttir, A., Miller, G. H., Axford, Y., and **Ólafsdóttir**, S., 2009: Holocene and latest Pleistocene climate and glacier fluctuations in Iceland. *Quaternary Science Reviews*, 28: 2107–2118.

Ghil, M., Allen, M. R., Dettinger, M. D., Ide, K., Kondrashov, D., Mann, M. E., Roberston, A. W., Saunders, A., Tian, Y., Varadi, F., and Yiou, P., 2002: Advanced spectral methods for climatic time series. *Reviews of Geophysics*, 40(1): 3-1 to 3-41, doi: http://dx.doi.org/10.1029/2000RG000092.

Gilbert, R., 1990: Rafting in glacimarine environments. *In* Dowdeswell, J. A., Scourse, J. D. (eds.), *Glacimarine Environments: Processes and Sediments*. Geological Society, London, Special Publications, 53: 105–120.

Haggerty, S. E., 1976: Opaque mineral oxides in terrestrial igneous rocks. *In* Rumble, D., (ed.), *Oxide Minerals*. Reviews in Mineralogy, Vol. 3: 101–300.

Hammer, Ø., Harper, D. A. T., and Ryan, P. D., 2001: PAST: paleontological statistics software package for education and data analysis. *Palaeontologia Electronica*, 4: 9 pp.

Hastings, A. D., 1960: Environment of Southeast Greenland. U.S. Army, Quartermaster Research and Engineering Command, Technical Report EP-140, 62 pp.

Hebbeln, D., and Wefer, G., 1991: Effects of ice coverage and ice-rafted material on sedimentation in the Fram Strait. *Nature*, 350: 409–411.

Hellmann, L., Tegel, W., Kirdyanov, A. V., Eggertsson, O., Esper, J., Agafonov, L., Nikolaev, A. N., Knorre, A. A., Myglan, V. S., Churakova (Sidorova), O., Weingruber, F. H., Nievergelt, D., Verstege, A., and Büntgen, U., 2015: Timber logging in Central Siberia is the main source for recent Arctic driftwood. *Arctic, Antarctic, and Alpine Research*, 47: 449–460.

Higgins, A. K., Gilotti, J. A., and Smith, P. M., 2008: *The Greenland Caledonides. Evolution of the Northeast margin of Laurentia*. Geological Society of America, Memoir 202: 368 pp.

Hubberten, H. W., 1995: Die Expedition ARKTIS-X/2 mit FS "Polarstern" 1994. *Ber. Polarforsch.*, 174: 186 pp., http://epic.awi.de/26352/1/BerPolarforsch1995174.pdf.

Iceland Meteorological Office, 1987: Sea ice off the Icelandic coasts, October 1986–September 1987. Icelandic Meteorological Office, p. 31.

Iceland Meteorological Office, 1988: Sea ice off the Icelandic coasts, October 1987–September 1988. Icelandic Meteorological Office, p. 45.

Jennings, A. E., Gronvold, K., Hilberman, R., Smith, M., and Hald, M., 2002a: High resolution study of Icelandic tephras in the Kangerlussuaq Trough, southeast Greenland, during the last deglaciation. *Journal of Quaternary Science*, 17: 747–757.

Jennings, A. E., Knudsen, K. L., Hald, M., Hansen, C.V., and Andrews, J. T., 2002b: A mid-Holocene shift in Arctic sea ice variability on the East Greenland shelf. *The Holocene*, 12: 49–58.

Jennings, A. E., Weiner, N. J., Helgad**ó**ttir, G., and Andrews, J. T., 2004: Modern foraminiferal faunas of the Southwest to Northern Iceland shelf: oceanographic and environmental controls. *Journal of Foraminiferal Research*, 34: 180–207.

Jennings, A. E., Hald, M., Smith, L. M., and Andrews, J. T., 2006: Freshwater forcing from the Greenland Ice Sheet during the Younger Dryas: evidence from Southeastern Greenland shelf cores. *Quaternary Science Reviews*, 25: 282–298.

Jennings, A. E., Andrews, J. T., and Wilson, L., 2011: Holocene environmental evolution of the SE Greenland Shelf north and south of the Denmark Strait: Irminger and East Greenland current interactions. *Quaternary Science Reviews*, 30: 980–998.

Jennings, A. E., Kelly, J., Shreve, B., Reed, M., and Andrews, J. T., 2013: Ice rafting events off central West Greenland: a record of ice sheet retreat from northern Baffin Bay? Geological Society America Programs with Abstracts, 45(7): Paper 39-13 (Poster).

Jennings, A. E., Thordarson, T., Zalzal, K., Stoner, J. F., Hayward, C., Geirsd**ó**ttir, A., and Miller, G. H., 2014: Holocene tephra from Iceland and Alaska record in SE Greenland Shelf sediments. *In* Austin, W. E. N., Abbott, P. M., Davis, S. M., Pearce, N. J. G., and Wastegard, S. (eds.), *Marine Tephrochronology*. Geological Society, London, Special Publications, 398: 157–193.

Jónsdóttir, I., and Sveinbjornsson, E., 2007: Recent variations in sea-ice extent off Iceland. *Jokull*, 57: 61–70.

Jónsdóttir, I. R., **Ólafsdóttir**, S., and Geirsd**ó**ttir, A., 2015: Marine climate variability from Amarfjorour, NW Iceland during the Medieval Warm period and early/middle Little Ice Age. *Jokull*, 65: 73–88.

Kantz, H., and Schreiber, T., 1997: *Nonlinear Time Series Analysis*. Cambridge: Cambridge University Press, 304 pp.

Khan, S. A., Aschwanden, A., Bjork, A. A., Wahr, J., Kjeldsen, K. K., and Kjaer, K. H., 2015: Greenland ice sheet mass balance: a review. *Reports on Progress in Physics*, 78(4): 046801, doi: http://dx.doi.org/10.1088/0034-4885/78/4/046801.

Kjeldsen, K. K., Korsgaard, N. J., Bjork, A. A., Khan, S. A., Box, J. E., Funder, S., Larsen, N. K., Bamber, J. L., Colgan, W., van den Broeke, M., Siggaard-Andersen, M. L., Nuth, C., Schomacker, A., Andresen, C. S., Willerslev, E., and Kjaer, K. H., 2015: Spatial and temporal distribution of mass loss from the Greenland Ice Sheet since AD 1900. *Nature*, 528: 396–400, doi: http://dx.doi.org/10.1038/nature16183.

Koch, L., 1945: The East Greenland Ice. *Meddelelser om Grønland*, 130(3): 346 pp.

Kraus, W., 1958: Die hydrographischen Untersuchungen mit "Anton Dohrn" auf dem ost- westgronlandischen Schelf im September–Oktober 1955. *Ber. Disch. Wiss. Komm. Meresforsch.*, 15: 77–104.

Kristjansd**ó**ttir, G. B., Moros, M., Andrews, J. T., and Jennings, A. E., 2016: Holocene Mg/Ca, alkenones, and light stable isotope measurements on the outer North Iceland shelf (MD99-2269): a comparison with other multi-proxy data and subdivision of the Holocene. *The Holocene*, 27(1): 52–62.

kspectra, 2015: kSpectra Toolkit for Mac OS X! Small signal finder. Happy fishing in Ocean of Noise! http://www.spectraworks.com/web/products.html.

Labeyrie, L., Jansen, E., and Cortijo, E., 2003: Les rapports de campagnes à la mer MD114/IMAGES V. Plouzané, France: Institut Polaire Français, Réf: OCE/2003/02, 850 pp.

Larsen, M., Hamberg, L., Olaussen, S., Norgaard-Pedersen, N., and Stemmerik, L., 1999: Basin evolution in southern East Greenland: an outcrop analog for Cretaceous–Paleogene basins on the North Atlantic volcanic margins. *AAPG Bulletin*, 83: 1236–1261.

Lysa, A., and Landvik, J.Y., 1994: The lower Jyllandselv succession: evidence for three Weichselian glacier advances over coastal Jameson Land, East Greenland. *Boreas*, 23: 432–446.

Malmberg, S.-A., 1985: The water masses between Iceland and Greenland. *Journal of Marine Research Institute*, 9: 127–140.

Massé, G., Rowland, S. J., Sicre, M.-A., Jacob, J., Jansen, E., and Belt, S. T., 2008: Abrupt climate changes for Iceland during the last millennium: evidence from high resolution sea ice reconstructions. *Earth and Planetary Science Letters*, 269: 565–569.

McBirney, A. R., and Noyes, R. M., 1979: Crystallization and layering of the Skaergaard Intrusion. *Journal of Petrology*, 20: 487–554.

Meier, W., Stroeve, J., Fetterer, F., and Knowles, K., 2005: Reductions in Arctic Sea ice cover no longer limited to summer. *EOS, Transactions of the American Geophysical Union*, 86(36): 326.

Miller, G. H., Geirsd**ó**ttir, A., Zhong, Y. F., Larsen, D. J., Otto-Bliesner, B. L., Holland, M. M., Bailey, D. A., Refsnider, K. A., Lehman, S. J., Southon, J. R., Anderson, C., Bjornsson, H., and Thordarson, T., 2012: Abrupt onset of the Little Ice Age triggered by volcanism and sustained by sea-ice/ocean feedbacks. *Geophysical Research Letters*, 39: Article L02708, doi: http://dx.doi.org/10.1029/2011gl050168.

Miller, R. L. and Kahn, J. S. 1962: *Statistical Analysis in the Geological Sciences*. New York: John Wiley and Sons, Inc., 483 pp.

Moore, G. W. K., and Renfrew, I. A., 2014: A new look at Southeast Greenland barrier winds and katabatic flow. *U.S. CLIVAR Variations Newsletter*, 12(2): 1–19, 3 pp. figures, http://polarmet.osu.edu/ASR/asr_moore_clivar_2014.pdf.

Müller, J., Wagner, A., Fahl, K., Stein, R., Prange, M., and Lohmann, G., 2011: Towards quantitative sea ice reconstructions in the northern North Atlantic: a combined biomarker and numerical modeling approach. *Earth and Planetary Science Letters*, 306: 137–148.

Müller, J., Werner, K., Stein, R., Fahl, K., Moros, M., and Jansen, E., 2012: Holocene cooling culminates in sea ice oscillations in Fram Strait. *Quaternary Science Reviews*, 47: 1–14.

Nam, S.-I., Stein, R., Grobe, H., and Hubberten, H., 1995: Late Quaternary glacial/interglacial changes in sediment composition at the East Greenland continental margin and their paleoceanographic implications. *Marine Geology*, 122: 243–262.

Neff, U., Burns, S. J., Mangini, A., Mudelsee, M., Fleitmann, D, and Matter, A., 2001: Strong coherence between solar variability and the monsoon in Oman between 9 and 6 kyr ago. *Nature*, 411: 290–293.

Ogilvie, A. E. J., 1996: Sea-ice conditions off the coasts of Iceland A.D. 1601–1850 with special reference to part of the Maunder Minimum period (1675–1715). *In* Pedersen, E. S. (ed.), *North European Climate Data in the Latter Part of the Maunder Minimum Period A.D. 1675–1715*. Stavanger, Norway: Archaeological Museum of Stravanger, 9–12.

Ogilvie, A. E. J., 1997: Fisheries, climate and sea ice in Iceland: an historical perspective. *In* Vickers, D. (ed.), *Marine Resources and Human Societies in the North Atlantic since 1500*. St. John's, Newfoundland: Institute of Social and Economic Research, Memorial University, 69–87.

Ogilvie, A. E. J., and Jónsdóttir, I., 2000: Sea ice, climate, and Icelandic fisheries in the eighteenth and nineteenth centuries. *Arctic*, 53: 383–394.

Ólafsdóttir, S., 2004: *Currents and Climate on the Northwest Shelf of Iceland during the Deglaciation: High-Resolution Foraminiferal Research*. Ph.D. dissertation, Department of Geosciences, University of Iceland, Reykjavik, 117 pp.

Ólafsdóttir, S., Jennings, A. E., Geirsd**ó**ttir, A., Andrews, J., and Miller, G. H., 2010: Holocene variability of the North Atlantic Irminger current on the south- and northwest shelf of Iceland. *Marine Micropaleontology*, 77: 101–118.

Paillard, D., Labeyrie, L., and Yiou, P., 1996: Macintosh program performs time-series analysis. *EOS, Transactions of the American Geophysical Union*, 77(39): 379.

Perner, K., Moros, M., Lloyd, J. M., Jansen, E., and Stein, R., 2015: Mid to late Holocene strengthening of the East Greenland Current linked to warm subsurface Atlantic waters. *Quaternary Science Reviews*, 129: 296–307.

Perner, K., Jennings, A. E., Moros, M., Andrews, J. T., and Wacker, L., 2016: Millennial scale mid to late Holocene oscillation of the East Greenland and Irminger Current on the south-eastern Greenland shelf. *Journal of Quaternary Science*, 31: 472–483.

Prins, M. A., Bouwer, L. M., Beets, C. J., Troelstra, S. R., Weltje, G. J., Kruk, R. W., Kruijpers, A., and Vroon, P. Z., 2002: Ocean circulation and iceberg discharge in the glacial North Atlantic: inferences from unmixing of sediment sizes. *Geology*, 30: 555–558.

Reeh, N., 2004: Holocene climate and fjord glaciations in Northeast Greenland: implications for IRD deposition in the North Atlantic. *Sedimentary Geology*, 165: 333–342.

Reeh, N., Thomsen, H. H., Higgins, A. K., and Weidick, A., 2001: Sea ice and the stability of north and northeast Greenland floating glaciers. *Annals of Glaciology*, 33(1): 474–480.

Reimnitz, E., Marincovich, L., Jr., McCormick, M., and Briggs, W. M., 1992: Suspension freezing of bottom sediment and biota in the Northwest Passage and implications for Arctic Ocean sedimentation. *Canadian Journal of Earth Sciences*, 29: 693–703.

Reimnitz, E., Clayton, J. R., Kempema, E. W., Payne, J. R., and Weber, W. S., 1993: Interaction of rising frazil with suspended particles: tank experiments with applications to nature. *Cold Regions Science and Technology*, 21: 117–135.

Rennermalm, A. K., Wood, E. F., Weaver, A. J., Eby, M., and Déry, S. J., 2007: Relative sensitivity of the Atlantic meridional overturning circulation to river discharge into Hudson Bay and the Arctic Ocean. *Journal of Geophysical Research*, 112(G4): G04S48, doi: http://dx.doi.org/10.1029/2006JG000330.

Ruddiman, W. F., 1977a: Late Quaternary deposition of ice-rafted sand in the sub-polar North Atlantic (lat 40° to 65°N). *Geological Society of America Bulletin*, 88: 1813–1827.

Ruddiman, W. F., 1977b: North Atlantic ice-rafting: a major change at 75,000 years before the present. *Science*, 196(4295): 1208–1211.

Rudels, B., Fahrbach, E., Meincke, J., Budéus, G., and Eriksson, P. 2002: The East Greenland Current and its contribution to the Denmark Strait overflow. *ICES Journal of Marine Science*, 59: 1133–1154.

Schmith, T., and Hanssen, C., 2003: Fram Strait ice export during the nineteenth and twentieth centuries reconstructed from a multiyear sea ice index from Southwestern Greenland. *Journal of Climate*, 16: 2782–2791.

Seale, A., Christoffersen, P., Mugford, R. I., and O'Leary, M., 2011: Ocean forcing of the Greenland Ice Sheet: calving fronts and patterns of retreat identified by automatic satellite monitoring of eastern outlet glaciers. *Journal of Geophysical Research–Earth Surface*, 116(F3): 16 pp., doi: http://dx.doi.org/10.1029/2010JF001847.

Shepherd, A. P., and Wingham, D. J., 2007: Recent sea-level contributions of the Antarctic and Greenland ice sheets. *Science*, 315(5818): 1529–1532.

Simon, Q., 2007: Analyse sédimentologique et isotopique (Nd and Pb) d'une carotte sédimentaire prélevée dans le Détroit du Danemark (MD99-2322) Implication sur l'évolution de la circulation océanique profonde au cours de l'Holocène. *Oceanography*, Liège, 92.

Smith, L. M., and Andrews, J. T., 2000: Sediment characteristics in iceberg dominated fjords, Kangerlussuaq region, East Greenland. *Sedimentary Geology*, 130: 11–25.

Stein, A. B., 1996: *Seismic Stratigraphy and Seafloor Morphology of the Langerlussuaq Region, East Greenland: Evidence for Glaciations to the Continental Shelf Break during the Late Weischelian Age and Earlier*. Ph.D. dissertation, Department

of Geological Sciences, University of Colorado, Boulder, 293 pp.

Stein, R., 2008: *Arctic Ocean Sediments. Processes, Proxies, and Paleoenvironment*. New York: Elsevier, 608 pp.

Stein, R., Grobe, H., Hubberten, H., Marienfeld, P., and Nam, S., 1993: Latest Pleistocene to Holocene changes in glaciomarine sedimentation in Scoresby Sund and along the adjacent East Greenland continental margin: preliminary results. *Geo-Marine Letters*, 13: 9–16.

Stoner, J. S., Jennings, A. E., Kristjansd**ó**ttir, G. B., Andrews, J. T., Dunhill, G., and Hardard**ó**ttir, J., 2007: A paleomagnetic approach toward refining Holocene radiocarbon based chronostratigraphies: Paleoceanographic records from North Iceland (MD99-2269) and East Greenland (MD99-2322) margins. Paleoceanography, 22(1): 23 pp., PA1209, doi: http://dx.doi.org/10:1029/2006PA001285.

Straneo, F., and Heimbach, P., 2013: North Atlantic warming and the retreat of Greenland›s outlet glaciers. *Nature*, 504: 36–43.

Strikis, N. M., Cruz, F. W., Cheng, H., Karmann, I., Edwards, R. L., Vuille, M., Wang, X. F., de Paula, M. S., Novello, V. F., and Auler, A. S., 2011: Abrupt variations in South American monsoon rainfall during the Holocene based on a speleothem record from central-eastern Brazil. *Geology*, 39: 1075–1078.

Stroeve, J. C., Serreze, M. C., Holland, M. M., Kay, J. E., Malanik, J., and Barrett, A. P., 2012: The Arctic's rapidly shrinking sea ice cover: a research synthesis. *Climatic Change*, 110: 1005–1027.

Sutherland, D. A., and Pickart, R. S., 2008: The East Greenland Coastal Current: structure, variability, and forcing. *Progress in Oceanography*, 78: 58–77.

Syvitski, J. P. M., Andrews, J. T., and Dowdeswell, J. A., 1996: Sediment deposition in an iceberg-dominated glacimarine environment, East Greenland: basin fill implications. *Global and Planetary Change*, 12: 251–270.

Syvitski, J. P. M., Stein, A., Andrews, J. T., and Milliman, J. D., 2001: Icebergs and seafloor of the East Greenland (Kangerlussuaq) continental margin. *Arctic, Antarctic, and Alpine Research*, 33: 52–61.

Thordard**ó**ttir, T., 1984: Primary production north of Iceland in relation to water masses in May–June 1970–1980. International Council for the Exploration of the Sea, C.M. 1984/L20, 1–17.

Thordard**ó**ttir, T., 1986: Timing and duration of spring blooming south and southwest of Iceland. *In* Skreslet, S. (ed.), *The Role of Freshwater Outflow in Coastal Marine Ecosystems*. NATO ASI Series G7. Berlin: Springer-Verlag, 345–360.

Thors, K., 1974: I. *Sediments of the Vestfirdir Shelf, NW Iceland, and II. Geology of the Ulfarsfell Area, SW Iceland*. Ph.D. dissertation, University of Manchester, U.K., 167 pp.

Våge, K., Pickart, R. S., Spall, M. A., Moore, G. W. K., Valdimarsson, H., Torres, D. J., Erofeeva, S. Y., and Nilsen, J. E. O., 2013: Revised circulation scheme north of the Denmark Strait. *Deep Sea Research Part I: Oceanographic Research Papers*, 79: 20–39.

van den Broeke, M., Bamber, J., Ettema, J., Rignot, E., Schrama, E., van de Berg, W. J., van Meijgaard, E., Velicogna, I., and Wouters, B., 2009: Partitioning recent Greenland mass loss. Science, 326(5955): 984–986.

Vautard, R., Yiou, P., and Ghil, M., 1992: Singular-spectrum analysis: a toolkit for short, noisy chaotic signals. *Physica, D: Nonlinear Phenomena*, 58: 95–126.

Verplanck, E. P., Farmer, G. L., Andrews, J., Dunhill, G., and Millo, C., 2009: Provenance of Quaternary glacial and glacimarine sediments along the southeast Greenland margin. *Earth and Planetary Science Letters*, 286: 52–62.

Wagner, G., Beer, J., Masarik, J., Muscheler, R., Kubik, P. W., Mende, W., Laj, C., Raisbeck, G. M., and Yiou, F., 2001: Presence of the solar deVries cycle (~205 years) during the last ice age. *Geophysical Research Letters*, 28: 303–306.

Wahsner, M., Müller, C., Stein, R., Ivanov, G., Levitan, M., Shelekhova, E., and Tarasov, G., 1999: Clay-mineral distribution in surface sediments of the Eurasian Arctic Ocean and continental margin as indicator for source areas and transport pathways: a synthesis. *Boreas*, 28: 215–233, doi: http://dx.doi.org/10.1111/j.1502-3885.1999.tb00216.x.

Wallevik, J. E., and Sigurjónsson, H., 1998: The Koch Index: Formulation, Corrections and Extension. Reykjavík: Icelandic Meteorological Office Report, 13 pp., map, http://www.vedur.is/media/vedurstofan/utgafa/greinargerdir/1998/98035.pdf.

Warren, C. R., 1992: Iceberg calving and the glacioclimatic record. *Progress in Physical Geography*, 16: 253–282.

White, L. F., Bailey, I., Foster, G. L., Allen, G., Kelley, S. P., Andrews, J. T., Hogan, K., Dowdeswell, J. A., and Storey, C. D., 2016: Tracking the provenance of Greenland-sourced, Holocene aged, individual sand-sized ice-rafted debris using the Pb-isotope compositions of feldspars and $^{40}Ar/^{39}Ar$ ages of hornblendes. *Earth and Planetary Science Letters*, 433: 192-203.

Xiao, X., Fahl, K., Müller, J., and Stein, R., 2015: Sea-ice distribution in the modern Arctic Ocean: biomarker records from trans-Arctic Ocean surface sediments. *Geochimica et Cosmochimica Acta*, 155: 16–29.

MS submitted 27 January 2017
MS accepted 25 August 2017

Appendix

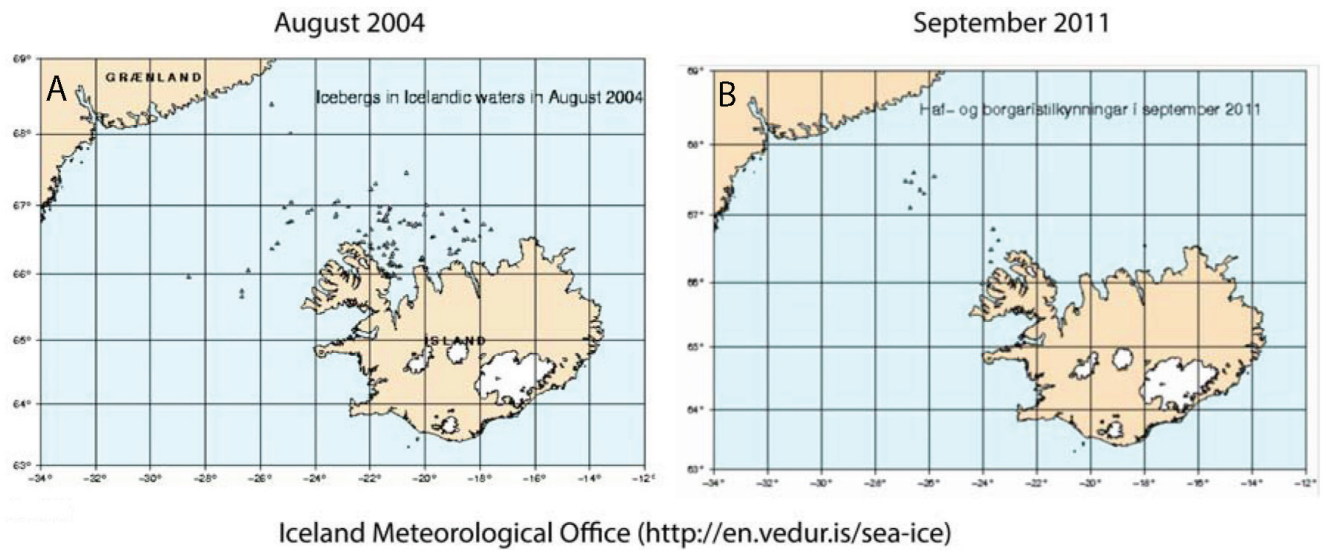

FIGURE A1. (A) Distribution of icebergs in Icelandic waters in August 2004; (B) distribution of icebergs in Icelandic waters in September 2011.

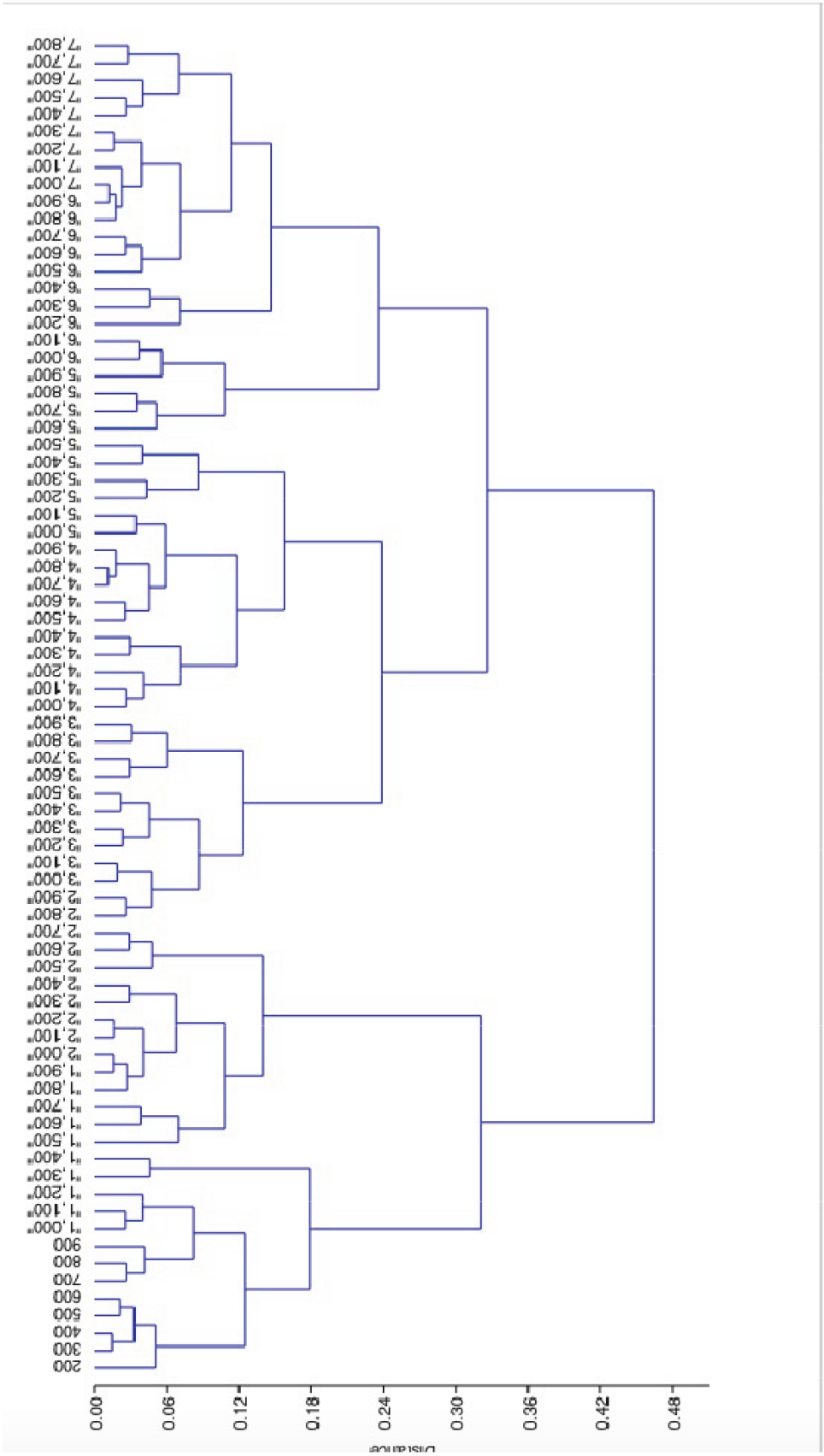

FIGURE A2. Constrained clustering of the proxies from 2322 plotted for the last 8000 cal. yr B.P.